Silesian University in Opava
Institute of Physics in Opava

SILESIAN UNIVERSITY
INSTITUTE OF PHYSICS IN OPAVA

Thin accretion disks

Part I: Basic concepts and solutions

Dr. Miljenko Čemeljić

Opava, 2022

OPEN UNI - zlepšení otevřenosti a atraktivnosti studia na SU,
CZ.02.2.69/0.0/0.0/18_056/0013364

EUROPEAN UNION
European Structural and Investment Funds
Operational Programme Research,
Development and Education

MINISTRY OF EDUCATION, YOUTH AND SPORTS

Contents

1 Introduction to accretion **7**
- 1.1 How we arrived to accretion 7
- 1.2 Energetics of accretion 7
- 1.3 Eddington limit 8
- 1.4 Spherical accretion 9
- 1.5 Disk accretion 9
- 1.6 Viscosity 10
- 1.7 Role of turbulence 12

2 Steady accretion disk solutions **13**
- 2.1 Perturbative solutions for the disk . . 15
- 2.2 Stationary thin disk 16
- 2.3 Shakura & Sunyaev viscous alpha disk 18
  - 2.3.1 Surface density 19
  - 2.3.2 Disk height 20
  - 2.3.3 Mass density 20
  - 2.3.4 Temperature 21
  - 2.3.5 Optical depth 21
  - 2.3.6 Viscosity 21
  - 2.3.7 Velocity 21
- 2.4 Working of MRI in the disk 22
- 2.5 Self-gravity in the disk 23

3 General accretion disk solutions **25**
- 3.1 Urpin's and Regev's vertically averaged solutions 25
- 3.2 Kluźniak-Kita 3D global solution . . . 26
  - 3.2.1 B0=0 solutions 32
  - 3.2.2 Analytical expressions from the numerical solutions . . . 38
- 3.3 Comparison of the analytical and numerical solutions 42
- 3.4 Difference between numerical and analytical solutions 44

Preface

Stars are made of the material collected from the initial cloud of matter, which is falling towards the common center of gravity. According to the law of angular momentum conservation, the material at large radius brings inwards its angular momentum-speeding-up the rotation of the object it is building.

Since the stars are in general not fast rotators, there must be a mechanism which expels the angular momentum outwards from the central object, while gathering mass inwards. Simple theoretical arguments of such processes of accretion of matter on the were extended throughout XX ct., and were increasingly corroborated (or falsified) by the subsequent numerical simulations, which are needed to address the increasingly detailed questions, posed by the ever more precise observations.

The observational evidence was mainly available in the field of close binary stars, so this is where the need for most detailed models came first. The unprecedented wealth of data from the survey of fast series of spectrographic data in "strange" stars like ϵ Aurigae and β Lyrae, gathered by Struve and collaborators, initiated what Popper (1970) [HS70] called "Struve revolution". The whole concept of stability of such systems changed, so that about mid-XX ct. streams or rings of gas, exploding gas envelopes, Roche equipotential surfaces and thick gas disks were included in the models, tested with observational data.

Similar concepts took hold in the other fields of astronomy, for explaining the inner workings of the active galactic nuclei, centers of galaxy clusters and quasars.

When their radial extension is compared to height, many of such disks are thin, with height typically less than 1/10 of the radial distance from the central object. This offered some simplification in the mathematical analysis, as equations could be simplified by taking into account the height ratio as a small parameter in the analysis. This is the approach in which the analytical full 3D purely hydrodynamical solution (Kluźniak & Kita disk), which we present here, is obtained. We also present our magnetic extension of this solution.

In this series of lectures, we review methods from some seminal works on thin accretion disk, and offer some insights in solutions of the encountered problems, both in purely hydrodynamic and magnetohydrodynamic treatment. To assist the reader, we often solve the equations in the great detail. The present volume is dedicated to the theoretical concepts, and the second volume will detail the numerical simulations of a thin accretion disk.

Lectures were delivered at the Silesian University in Opava in February/March 2022. Author is grateful to students and the host, Institute of Physics in Opava, for a friendly and motivating environment. The work in Opava was supported by the Czech ESF projects No. CZ.02.2.69/0.0/0.0/18_054/0014696, and author was also funded by a Polish NCN grant No. 2019/33/B/ST9/01564.

PhD students in CAMK Warsaw, Fatemeh Kayanikhoo and Angelos Karakonstantakis, are thanked for reviewing the final draft, and Angelos in addition for inputing the step-by-step equations for SS73 solutions.

Chapter 1

Introduction to accretion

Accretion is a process of mass collection onto a (usually rotating) central body, where a particle or a fluid element moving at some orbit transfers part of its energy and angular momentum to its surrounding. More general, it can be described as inward motion of matter because of the gravitational force-this definition we need to include the simplest case which we will first study, the spherical (Bondi) accretion.

Gravity was the first force to be studied extensively, in mechanics, our first applied science. In astronomy it was for long the only computed force, by Newton. It was The Force of celestial motions, until we started computing the machinery of stellar power. Then it showed gravity is not enough- electromagnetic interactions (chemistry) were also helpless - Sun burning coal would expire practically on our eyes. Nuclear forces explained the powering of stars, but gravity made a comeback when we understood that the Sun-like stars are weaklings in comparison to a much larger energy output of stellar compact objects, black holes and galactic nuclei.

1.1 How we arrived to accretion

Historically, accretion was first considered as a relevant process in the close binaries: after collecting a wealth of spectrographic data by Struve and collaborators, it became obvious that simple models of stellar stability are insufficient to explain the spectral features-theoretical curves were too smoothed by the simplifications, and observational curves were not smooth at all! Introducing more physical processes into astrophysics of stars was called "Struve revolution" by Popper[1] in 1970 ([HS70]): To explain the spectral features, hence the energy and angular momentum evolution in the "peculiar stars" - which mostly showed to be close binaries, astronomers around the middle of XX century had to include the streams of matter, gas rings, Roche's equipotential surfaces, and finally Huang [Hua63] included a thick disk. Gradually, with increase in quality of data, similar concepts were introduced in the objects on other scales, like active galactic nuclei (AGNs), quasars, and centers of clusters of galaxies. Astrophysics of accretion could start!

1.2 Energetics of accretion

When I said that with accretion gravity made a comeback, I should say that it made it with a boom! - accretion is by far the most efficient way of extracting energy out of the matter we know: it yields about 10 times more energy than nuclear fusion!

We can show it in a back-of-the-envelope calculation for the luminosity of the disk acquired by the infall

[1] Not the philosopher of science, Karl Popper, but astrophysicist Daniel M. Popper, from L.A., University of California.

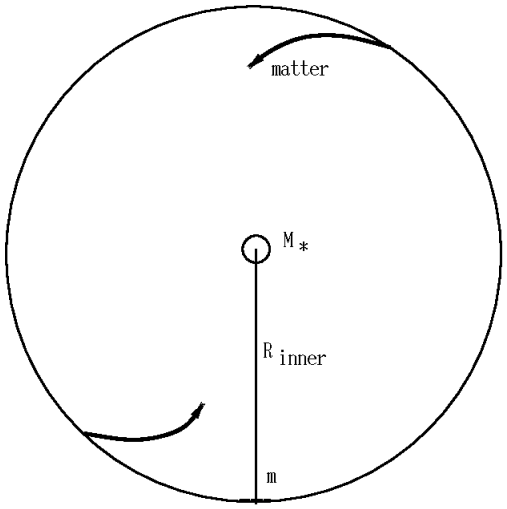

Figure 1.1: Matter infalling from inifinity onto a central body.

of material from the large distance onto a central object. The luminosity L is

$$L = \frac{dE}{dt},\ where\ E = \frac{m}{2}(v_\infty^2 - v_{\mathrm{K}i}^2),\ with\ v_{\mathrm{K}i} = \sqrt{\frac{GM_\star}{R_i}} \tag{1.1}$$

the Keplerian velocity at the orbit R_i, and v_∞ is the escape velocity of a mass m. It will bring to the orbit R_i the same energy which would be needed to launch it from that orbit into the "infinity" at R_∞, beyond the gravitational pull of the central object:

$$\frac{mv_\infty^2}{2} = \frac{GM_\star m}{R_i} - \frac{GM_\star m}{R_\infty}, \tag{1.2}$$

$$v_\infty = \sqrt{\frac{2GM_\star}{R_i}} \text{ so that } L = \frac{GM_\star \dot{m}}{2R_i}. \tag{1.3}$$

In the literature, one can find various numbers for the efficiency of accretion, I list some below, but what is meant by "efficiency"? It is the power P available at a given mass accretion rate $\dot{m}$ onto an object of radius R: $P = \dot{m}GM/R$. This power is usually dissipated away through radiation, otherwise there would be no accretion- and the produced heat would push the matter away.

For a black hole of mass $M_\star$ with a Schwarzschild radius $R_S = 2GM_\star/c^2$ we obtain the luminosity $L = \dot{m}R_S c^2/(4R_i)$, if the disk ends at $3R_S$ above the center of black hole, we obtain $L = \dot{m}c^2/12$ which is 8% of the rest mass energy of the accreted mass. In the nuclear fusion we obtain typically 1% of the rest mass energy, so accretion provides 10 times more efficient energy conversion than fusion!

Some examples of efficiency: Pair annihilation: $\eta = 1$; Nuclear (H) fusion: $\eta \sim 10^{-4}$; Accretion efficiency η onto Earth: 10^{-9}, Sun: 10^{-6}, white dwarf: 10^{-4}, neutron star: 10^{-1}.

Accretion efficiency $\eta = GM_\star/(Rc^2)$ onto a black hole (an object without a hard surface) depends on the details of accretion flow and spin of BH: $0.057 < \eta < 0.42$ for a thin accretion disk around black hole.

1.3 Eddington limit

What is the maximum luminosity at which matter still can be accreted[2]?

[2]This means that gravitational force on a chunk of fluid still just exceeds the radiation pressure

Simplest case is radial accretion onto a mass point M. If medium is fully ionised gas of electrons and protons, and we assume Compton scattering with the simplest radiation pressure

$$F_{\rm rad} = +\frac{\sigma_{\rm T}}{c}\frac{L}{4\pi r^2} \text{ and } F_{\rm g} = -m_{\rm p}\frac{GM}{r^2} \tag{1.4}$$

from $F_{rad} = F_{\rm g}$ we get that $L_{\rm Edd} = 4\pi GMm_{\rm p}c/\sigma_{\rm T}$. I list few Eddington luminosities: solar mass NS: $L_{\rm Edd} = 1.3 \times 10^{38}(M/M_{\odot})$erg/s ; supermassive BH: $1.3 \times 10^{46}(M/10^8 M_{\odot})$erg/s.

Eddington mass accretion rate is $\dot{m}_{\rm Edd} = L_{\rm Edd}/(\eta c^2)$.

Usually it is said that the accretion is not possible if $L > L_{Edd}$ but there are cases when it is not true, and they are very interesting cases of supernovae and non-spherical accretion cases in disks and jets.

1.4 Spherical accretion

H. Bondi [Bon52] gave an analytical solution for the spherically symmetric, steady-state accretion flow of an infinite gas cloud onto a point mass, in the Newtonian approach. Such model was later extended, to be applied from the study of star formation to cosmology.

Bondi considered adiabatic ($p \sim \rho^{\gamma}$) accretion of gas. Far from central mass, gas elements move in dependence of their thermal energy only, so that with gas temperature T_{inf} with sound speed $c_{\rm s}$ we can say that at some critical distance from the central mass r_{cr} the escape velocity is equal to the speed velocity: $r_{cr} = 2GM/c_{\rm s}^2$.

For $r < r_{cr}$ material falls freely onto the central mass, and for the density above the radius $r_{\rm cr}$, ρ_{inf} we can write the infalling mass $\dot{M} = 4\pi G^2 M^2 \rho_{inf}/c_{\rm s}^2$.

Hydrostatic equilibrium gives $\rho \sim r^{-3/2}$ (with $\gamma = 5/3$) and temperature $T \sim r^{3(1-\gamma)/2}$. Infalling gas reaches speed of sound at a distance $r_{\rm s}$ from the center. We find $r_{\rm s} = \frac{1}{4}(5-3\gamma)GM/c_{\rm s}^2$.

1.5 Disk accretion

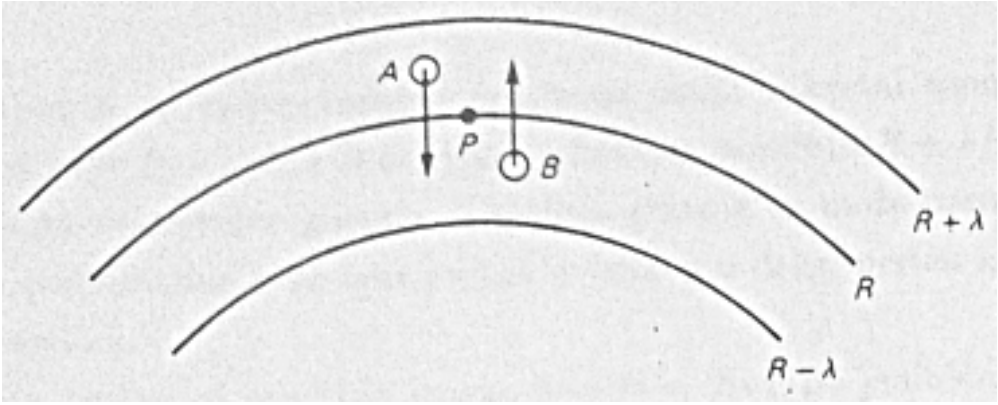

Figure 1.2: Two neighbor rings in the disk.

Let us take another view on accretion: material point orbiting around a center of mass interacts with its surrounding, transferring part of its energy and angular momentum. Consequence of such scenario is a slow spiral-in of the mass point. Energy which can be extracted is equal to the bonding energy of the smallest orbit: $E_{acr} = GMm/R$, see the back of the envelope calculation.

We consider rotating volume of gas with angular momentum L in cylindrical coordinates (R, φ, z), with z parallel to the axis of rotation. We further assume that distribution of L between the gas particles is much

slower than radiation transfer and rotation, so that L of the particle with mass m remains constant, but its kinetic and internal energy are distributed to other particles by collisions, shocks and radiation. For the constant L the minimal energy is for the circular orbit ⇒ we obtain the thin disk in which particles rotate with $v_\varphi = R\Omega(R)$ and we can write, with the potential Φ: $F_\mathrm{g} = ma = mv_\varphi^2/R = -d\Phi/dR = F_\mathrm{cf}$.

If there is a process counteracting the spread of particles (as viscosity), energy spreads through the system by heat, and escapes from the system by radiation. As a consequence, mass particle will orbit at smaller R, we can understand this as transformation of the orbital energy into radiation energy. With the gas surface density S(R,t) and radial velocity $v_\mathrm{r}(R,t)$, we observe the element of gas with inner radius R and outer $R+\Delta R$. Mass of such ring is $\Delta m = 2\pi R\cdot\Delta R\cdot S$, angular momentum $\boldsymbol{L} = \boldsymbol{R}\times\boldsymbol{p}$, where for angle of 90° between R and p we can write $L = Rmv_\varphi$, and in fact we can write, with $L = mR^2\Omega$, that the angular momentum of such ring is $2\pi R\Delta RSR^2\Omega$. Change of mass of such a ring is equal to the fluxes in and out from the neighboring rings (positive sign means the flow is directed away from the origin):

$$\begin{aligned}\frac{\partial}{\partial t}\Delta m = \mathrm{flux}(R) - \mathrm{flux}(R+\Delta R) = \\ v_r(R,t)\cdot 2\pi RS(R,t) - v_r(R+\Delta R,t)\cdot 2\pi(R+\Delta R)S(R+\Delta R,t) = \\ v_r(R,t)\cdot 2\pi RS(R,t) - v_r(R+\Delta R,t)\cdot 2\pi RS(R+\Delta R,t) - v_r(R+\Delta R,t)\cdot 2\pi\Delta RS(R+\Delta R,t) = \\ \text{with } \Delta R\to 0,\ \text{the } 3^{\mathrm{rd}}\text{ term} = 0 \text{ and } f(x+\Delta x) - f(x) = \Delta x\partial f(x)\partial x = -\Delta R\partial(2\pi RSv_\mathrm{r})/\partial R.\end{aligned}$$

Now we can write $\partial/\partial t(\Delta m)/\Delta R = -\partial/\partial R(2\pi RSv_\mathrm{r})$ and since $\Delta m/\Delta R = 2\pi RS$ and we stay, after divide by 2π, with $\partial/\partial t(RS) = -\partial/\partial R(RSv_\mathrm{r})$, $\partial R/\partial t = v_\mathrm{r}$. We can write further $v_\mathrm{r}S + R\partial S/\partial t = -v_\mathrm{r}S - R\partial/\partial R(Sv_\mathrm{r})$. Since $\partial/\partial R(RSv_\mathrm{r}) = v_\mathrm{r}S + R\partial/\partial R(Sv_\mathrm{r})$, we can write: $R\partial S/\partial t + \partial/\partial R(RSv_\mathrm{r}) = -v_\mathrm{r}S = 0$, as we are interested only in the change of mass.

Exercise: Do the derivation for conservation of the angular momentum of a ring, but now adding the term for transfer of angular momentum between the rings, because of viscous torques J, $\Delta R\partial J/\partial R$.

Solution:

$$\begin{aligned}\frac{\partial}{\partial t}(2\pi R\Delta RSR^2\Omega) = v_r(R,t)2\pi RS(R,t)R^2\Omega(R) = \\ -v_r(R+\Delta R,t)2\pi(R+\Delta R)S(R+\Delta R,t)(R+\Delta R)^2\Omega(R+\Delta R) + \frac{\partial J}{\partial R}\Delta R = \\ (R+\Delta R)^3 = R^3 + 3R^2\Delta R + 3R(\Delta R)^2 + (\Delta R)^3 \approx R^3 + 3R^2\Delta R = \\ v_r(R,t)2\pi RS(R,t)R^2\Omega(R+\Delta R) - 3v_r(R+\Delta R,t)2\pi\Delta RS(R+\Delta R,t)R^2\Omega(R+\Delta R) + \frac{\partial J}{\partial R}\Delta R.\end{aligned}$$

In the linear approximation, first two terms are $-\delta R\partial(2\pi v_\mathrm{r}RSR^2\Omega)/\partial R$ and we have $2\pi\Delta R\partial_t(RSR^2\Omega) = -\Delta R\partial_R(2\pi v_r rSR^2\Omega) - 3v_r 2\pi\Delta RSR^2\Omega + \partial_R J\Delta R$. We obtain

$$\frac{\partial R}{\partial t}SR^2\Omega + R^2\frac{\partial}{\partial R}(SR^2\Omega) = -\frac{\partial}{\partial R}(Rv_rSR^2\Omega) - 3v_rSR^2\Omega - \frac{1}{2\pi}\frac{\partial J}{\partial R}.$$

Again we discard constant 1st l.h.s and 2nd r.h.s. terms and write $\partial R/\partial t = v_\mathrm{r}$ to obtain:

$$R\frac{\partial}{\partial t}(SR^2\Omega) + \frac{\partial}{\partial R}(Rv_rSR^2\Omega) = \frac{1}{2\pi}\frac{\partial J}{\partial R}.$$

1.6 Viscosity

Now we will find the torque of two neighbor rings, as shown in Fig. 1.2. The speed of chaotic motion in the gas is $\tilde{v}$, and λ is the characteristic scale, which is also the mean free path. After exchange, element A will (in

average) have torque from the position $R-\lambda/2$, and element in B from $R+\lambda/2$. Material in chaotic movement does not transfer matter (in average =0), only the steady flow can. Transferred mass is $\partial m/\partial t = H\rho\tilde{v}$, where H is the disk height in z direction. For the accretion process essential is the difference in transported torques, and there is transport of torque because of chaotic motions. This is viscous torque. Observer in point P, rotating with $\Omega(R)$ sees fluid in $R-\lambda/2$ moving with speed $(R-\lambda/2)\Omega(R-\lambda/2)+\Omega(R)\lambda/2$. This gives the average flow of angular momentum by the unit angle directed outwards $\rho\tilde{v}HR[(R-\lambda/2)\Omega(R-\lambda/2)+\Omega(R)\lambda/2]$ and inwards $\rho\tilde{v}HR[R+\lambda\Omega(R-\lambda/2)/2-\Omega(R)\lambda/2]$. Torque on the outer ring by the inner ring is equal to total outwards torque. In the first order approximation we have:

$$\rho\tilde{v}HR\left\{\left[\left(R-\frac{\lambda}{2}\right)\Omega\left(R-\frac{\lambda}{2}\right)+\Omega(R)\frac{\lambda}{2}\right]-\left(R+\frac{\lambda}{2}\right)\Omega\left(R+\frac{\lambda}{2}\right)-\Omega(R)\frac{\lambda}{2}\right)\right]\right\}=$$
$$\rho\tilde{v}HR\left[R\Omega\left(R-\frac{\lambda}{2}\right)-R\Omega\left(R+\frac{\lambda}{2}\right)-\frac{\lambda}{2}\Omega\left(R-\frac{\lambda}{2}\right)-\frac{\lambda}{2}\Omega\left(R+\frac{\lambda}{2}\right)+2\Omega(R)\frac{\lambda}{2}\right]=-\lambda\rho\tilde{v}HR^2\frac{\partial\Omega}{\partial R},$$

since the first two terms in $\{\}$ give $-R\lambda\partial\Omega/\partial R$, and 3$^{\rm rd}$ and 4$^{\rm th}$ after $\lambda/2\to 0$ give $-\lambda/2\Omega(R)$.

For the whole ring we multiply the obtained result with $2\pi R$, and with the surface density $\rho H = S$ (from $\rho = m/V$, $S = m/A$ we divide with H, we have $S/H = m/(AH)$, r.h.s.=ρ) we obtain that the torque of the outer to the inner ring (- inner torque to the outer ring) is $J(R) = 2\pi R\nu SR^2\partial\Omega/\partial R$, where $\nu = \lambda\tilde{v}$ is the kinematic viscosity coefficient.

We had J=J(R,t), and with $R\partial\Omega/\partial R = A$ we have $J(R) = 2\pi R\nu SAR$, where νSA is a viscous force per unit angle. Now we can insert the obtained viscosity in the disk equations. We insert J into the equation we obtained from angular momentum conservation:

$$R\frac{\partial}{\partial t}(SR^2\Omega)+\frac{\partial}{\partial R}(Rv_rSR^2\Omega)=\frac{1}{2\pi}\frac{\partial J}{\partial R}. \tag{1.5}$$

We divide this with R and together with $R\partial S/\partial t+\partial/\partial R(RSvr)=0$ we can eliminate $v_{\rm r}$.

After the division with R, we can rewrite the equation as:

$$S\frac{\partial}{\partial t}(R^2\Omega)+R^2\Omega\frac{\partial S}{\partial t}+\frac{1}{R}R^2\Omega\frac{\partial}{\partial R}(SRv_r)+\frac{1}{R}SRv_r\frac{\partial}{\partial R}(R^2\Omega)=\frac{1}{R}\frac{\partial}{\partial R}(\nu SR^3\partial\Omega). \tag{1.6}$$

We write $R\partial_tS+\partial_R(RSvr)=0$ as $\partial_R(Rsv_{\rm r})=-R\partial_tS$ to obtain:

$$S\frac{\partial}{\partial t}(R^2\Omega)+R^2\Omega\frac{\partial S}{\partial t}-R^2\Omega\frac{\partial S}{\partial t}+\frac{1}{R}SRv_r\frac{\partial R^2\Omega}{\partial R}=\frac{1}{R}\frac{\nu SR^3\partial\Omega}{\partial R}. \tag{1.7}$$

In the first approximation $\boldsymbol{L}$ is a constant vector, and since $R^2\Omega$ is proportional to its length, we can discard the 1st term. We obtain:

$$v_r=\frac{\frac{1}{R}\frac{\partial}{\partial R}(\nu SR^3\frac{\partial\Omega}{\partial R})}{S\frac{\partial}{\partial R}(R^2\Omega)}. \tag{1.8}$$

Inserting it into $R\partial S/\partial t+\partial/\partial R(RSv_{\rm r})=0$ we have:

$$\frac{\partial S}{\partial t}=-\frac{1}{R}\frac{\partial}{\partial R}\left[RS\frac{\frac{1}{R}\frac{\partial}{\partial R}\left(\nu SR^3\frac{\partial\Omega}{\partial R}\right)}{S\frac{\partial}{\partial R}\left(R^2\Omega\right)}\right]=\frac{1}{R}\frac{\partial}{\partial R}\left\{\frac{\frac{\partial}{\partial R}\left[\nu SR^3\left(-\frac{\partial\Omega}{\partial R}\right)^2\right]}{\frac{\partial}{\partial R}\left(R^2\Omega\right)}\right\}. \tag{1.9}$$

With $F_{\rm g}=F_{\rm cf}$, in the potential of a point mass M we have $mv^2/R=GMm/R^2$ and $v_\varphi=\Omega R$, G=gravity

const., Keplerian $\Omega = (GM/R^3)^{1/2}$ and $d\Omega/dR = -3/2(GM/R^5)^{1/2}$. It follows:

$$\frac{\partial}{\partial R}\left(R^2\Omega\right) = \frac{\partial}{\partial R}\left(R^2\sqrt{GM}R^{-\frac{3}{2}}\right) = \frac{\partial}{\partial R}\left(\sqrt{GM}R^{\frac{1}{2}}\right) = \frac{1}{2}\sqrt{GM}R^{-\frac{1}{2}},$$

$$\frac{\partial S}{\partial t} = \frac{1}{R}\frac{\partial}{\partial R}\left[\frac{\frac{\partial}{\partial R}\left(\nu S R^3 \frac{3}{2}\sqrt{GM}R^{\frac{5}{2}}\right)}{\frac{1}{2}\sqrt{GM}R^{-1/2}}\right] = \frac{1}{R}\frac{\partial}{\partial R}\left[\frac{\frac{\partial}{\partial R}\left(\nu S \frac{3}{2}\sqrt{GM}R^{\frac{1}{2}}\right)}{\frac{1}{2}\sqrt{GM}R^{-1/2}}\right] = \frac{3}{R}\frac{\partial}{\partial R}\left[\sqrt{R}\frac{\partial}{\partial R}\left(\nu S\sqrt{R}\right)\right].$$

This is the diffusion equation for the surface density S: mass diffuses inwards, angular momentum outwards. Diffusion timescale is $t_{\rm visc} = R^2/\nu$.

1.7 Role of turbulence

We obtained the equation for surface density S. In general, ν depends on local conditions in the disk, and $\nu = \nu(S, R, t)$ so that we obtained nonlinear diffusion eq. for S. If ν depends on R only, equation is linear in S, even for the power of R - this was clear already in 1920-ies, Jeffreys 1924 [F J53], Weizsäcker in 1948 [Wei48].

Most of the mass moves towards the center, losing energy and torque. A tail of matter moves towards larger R to conserve the angular momentum. Matter from the initial ring arrives to the center, and total angular momentum is transported to large radii by a very small mass, compared to the disk mass. The disk slowly spreads outwards.

In 1973 Shakura & Sunyaev [SS73, hereafter SS73] gave a solution, parameterizing viscosity as $\nu = \alpha c_{\rm s} H$, where $\alpha < 1$ is a coefficient describing "turbulent viscosity". Usually $\nu \sim LV$, where L is characteristic scale, and v characteristic velocity of the turbulent eddies-so we assumed $L \sim H$ of the disk, and $V \sim c_{\rm s}$ (turbulence is usually assumed to be subsonic). In astrophysics we are usually dealing with large Reynolds numbers Re, defined through $Re = LV/\nu$, simply because of large L.

Re measures ratio of inertial to viscous forces, so in the disc we usually have proportionality with v_φ^2/R For $Re << 1$ viscous forces are dominating, and with $Re >> 1$ they are unimportant. In accretion discs usually $Re >> 10^{11}$ and we can not get much lower. Clue of the problem is exactly in so large Re: from experiments we know that fluids have some critical value $Re_{\rm c}$, at which the velocity becomes chaotic, so we have turbulence. Typical $Re_{\rm c} = 10^3$, so we can conclude that disc material is turbulent. Mathematically, viscous process is a diffusion process (of matter and angular momentum), this is the basics for our description.

There were many works on turbulence, but we still do not have the full understanding of the mechanism in accretion disks. Currently accepted paradigm is the one by [BH91], where magneto-rotational (MRI) turbulence is invoked. Recent works shows that to the first order, at least in some astronomical objects, outcomes of the viscous-alpha and MRI models are similar, see e.g. Mishra et al. (2020) [Mis+20]. It is still a developing topic.

Chapter 2

Steady accretion disk solutions

We will go through (sometimes painful) detail into the accretion disk equations. The obtained solution is still a starting point for explanation of the birth of stars and larger structures. Matter which we consider, when undergoing accretion, is gaseous, which means that interaction is by the collisions, not short distance forces. We use, as we did before, λ for the mean free path of the particles, $\tilde{v}$ for the mean velocity (velocities are measured in the comoving coordinates, and distributed following a Maxwell-Boltzmann distribution, which is dependent on the temperature, T), ρ for the mass density of gas. When observing the gas at scales $L >> \lambda$, we can consider it as a continuous fluid, with density, velocity and temperature defined in every point of the flow. The equations to describe such fluid are the equations of conservation of mass, momentum and energy.

Conservation of mass:

$$\frac{\partial \rho}{\partial t} + \nabla \cdot (\rho \boldsymbol{v}) = 0. \tag{2.1}$$

Conservation of momentum follows from the force acting on a fluid element:

$$-\oint P d\boldsymbol{n} = (\mathrm{G}auss - \mathrm{O}strogradski) = -\int_V \nabla P dV. \tag{2.2}$$

P is pressure, and the direction of the unit vector $\boldsymbol{n}$ is outwards from the volume.

Force acting on the unit volume element of the gas is $(-\nabla P)$, and its equation of motion we obtain from the 2$^{\mathrm{nd}}$ Newton's Law, multiplying it with the unit volume mass=density ρ and acceleration, so we can write:

$$\rho \frac{d\boldsymbol{v}}{dt} = -\nabla P. \tag{2.3}$$

Acceleration is also with respect to the comoving coordinates, not in the background rest system, so we have two parts in the velocity change in this equation: one is the change of velocity in the given point of space at a time interval dt: $\partial \boldsymbol{v}/\partial t dt$ and another is the difference in velocities at two points of space, distanced $\boldsymbol{r}$, through which the fluid flows during dt, what we can write as $d\boldsymbol{r}\nabla \boldsymbol{v}$, so we can write all together:

$$d\boldsymbol{v} = \frac{\partial \boldsymbol{v}}{\partial t} dt + d\boldsymbol{r} \nabla \cdot \boldsymbol{v} \, / \frac{1}{dt}, \tag{2.4}$$

$$\frac{d\boldsymbol{v}}{dt} = \frac{\partial \boldsymbol{v}}{\partial t} + \boldsymbol{v} \nabla \cdot \boldsymbol{v}. \tag{2.5}$$

When we insert it to the above equation of motion, we obtain:

$$\rho \frac{\partial \boldsymbol{v}}{\partial t} + \rho \boldsymbol{v} \nabla \cdot \boldsymbol{v} = -\nabla P. \tag{2.6}$$

General equation of motion should add the source term for the external forces acting on the system, we obtain the Euler equation:

$$\rho\frac{\partial \boldsymbol{v}}{\partial t} + \rho\boldsymbol{v}\nabla\cdot\boldsymbol{v} = -\nabla P + \boldsymbol{f}. \tag{2.7}$$

If we insert $\boldsymbol{f} = \rho\boldsymbol{g}$ for a gas in gravity field ($\boldsymbol{g}$ is the gravity acceleration), $\boldsymbol{f}$ could contain contributions from viscosity, external magnetic field etc. Momentum of the fluid element is $\rho\boldsymbol{v}$, conservation of the momentum is:

$$\frac{\partial}{\partial t}\rho\boldsymbol{v} = 0 = \frac{\partial \rho}{\partial t}\boldsymbol{v} + \rho\frac{\partial \boldsymbol{v}}{\partial t}. \tag{2.8}$$

For a stationary flow $\partial\rho/\partial t = 0$, and also the last derivative is zero, and we have

$$\rho\boldsymbol{v}\nabla\cdot\boldsymbol{v} + \nabla P - \rho\boldsymbol{g} = 0\ (A) \tag{2.9}$$

From

$$m\boldsymbol{g} = -GMm\boldsymbol{r}_0/r^2 \text{ is } \boldsymbol{g} = -GMm\boldsymbol{r}_0/r^2. \tag{2.10}$$

For the accretion onto spherical object of mass M, we choose spherical coordinates (r, θ, φ), radial component of the equation (A) is:

$$\rho v_{\rm r}\frac{1}{r^2}\left[\frac{d}{dr}(r^2 v_{\rm r})\right] + \frac{\partial P}{\partial r} + \rho\frac{GM}{r^2} = 0\ /\frac{1}{\rho} \tag{2.11}$$

$$\text{where } [] = 2rv_{\rm r} + r^2\partial v_{\rm r}/\partial r \text{ so we have} \tag{2.12}$$

$$\frac{2v_{\rm r}^2}{r} + v_{\rm r}\frac{\partial v_{\rm r}}{\partial r} + \frac{1}{\rho}\frac{\partial P}{\partial r} + \frac{GM}{r^2} = 0.\ (B) \tag{2.13}$$

From the continuity equation we have, for the stationary case with $\partial P/\partial t = 0$ that $\partial\rho/\partial t + \nabla(\rho v_{\rm r}) = 0$. For any vector $\boldsymbol{A}$ radial part is $\nabla\cdot\boldsymbol{A} = \frac{1}{r^2}[\frac{d}{dr}(r^2 A_{\rm r})]$ so we have $\rho\frac{1}{r^2}\frac{d}{dr}(r^2 v_{\rm r}) = 0/\int$, which means that $r^2 v_{\rm r} = const.$

Since $(-\rho v_{\rm r})$ is inflow mass flux, this constant must be related to mass flux, i.e. the accretion rate $\dot{M} = 4\pi r\rho(-v_{\rm r})$, since $r^2\cdot(inflow\ flux) = const = \dot{M}/(4\pi)$, for the whole sphere is $4\pi r^2\dot{M}\cdot(inflow\ flux)$. Now we insert $r^2 v_{\rm r} = -\dot{M}/(4\pi\rho)$ into the eq.(B) from above to obtain $v_{\rm r} = -\dot{M}/(4\pi\rho r^2)$, which in the limit $r \to 0$ gives $v_{\rm r} = 0$ and for the stationary spherical accretion we stay with

$$v_{\rm r}\frac{\partial v_{\rm r}}{\partial r} + \frac{1}{\rho}\frac{\partial P}{\partial r} + \frac{GM}{r^2} = 0. \tag{2.14}$$

Energy conservation:
The gas element energy is a sum of kinetic term $\rho v^2/2$ (by unit volume) and internal (thermal) energy $\epsilon\rho$ (where ϵ is the specific energy-by mass unit, dependent on temperature T). From the equipartition of energy we know that each degree of freedom has average energy of $kT/2$, so for a mono-atomic gas we have only 3 translational directions and we can write $\epsilon = 3kT/2$. Energy conservation equation we write similar to the mass conservation, adding source terms, depending on physics we include in our model. Instead of density ρ, now we conserve the kinetic and internal energy, and in the spatial derivative we will have work done by the pressure, $P\boldsymbol{v}$:

$$\frac{\partial}{\partial t}(\frac{1}{2}\rho v^2 + \rho\epsilon) + \nabla\cdot[(\frac{1}{2}\rho v^2 + \rho\epsilon + P)\boldsymbol{v}] - \boldsymbol{f}\boldsymbol{v} = 0, \tag{2.15}$$

and for a stationary case:

$$\rho\epsilon) + \nabla\cdot[(\frac{1}{2}\rho v^2 + \rho\epsilon + P)\boldsymbol{v}] = \boldsymbol{f}\boldsymbol{v}. \tag{2.16}$$

On the r.h.s. we can add the losses (with the - sign!) by radiation, heat etc. as the source terms inside the $-\nabla()$ term.

2.1 Perturbative solutions for the disk

Now we move to the perturbation method-we compute the perturbation in relation to the hydrostatic balance. We obtained

$$\begin{aligned} \nabla \cdot (\rho \boldsymbol{v}) &= 0 \\ \rho(\boldsymbol{v} \cdot \nabla)\boldsymbol{v} &= -\nabla P + \boldsymbol{f} \\ \nabla \cdot \left[\left(\frac{1}{2}\rho v^2 + \rho\epsilon + P \right) \boldsymbol{v} \right] &= \boldsymbol{f}\boldsymbol{v}, \end{aligned} \tag{2.17}$$

and with $v = 0$ in the hydrostatic case we stay only with

$$\nabla P = \boldsymbol{f}. \tag{2.18}$$

For the ideal gas, which we can assume everywhere except degenerate gas in some dense objects or near the centres of the normal stars, we have

$$P = \frac{\rho K T}{\mu m_{\mathrm{H}}}, \tag{2.19}$$

with $m_{\mathrm{H}} \sim m_{proton}$ the hydrogen atom mass, and μ is the average molecular mass in units of m_{H}, so that for completely ionized hydrogen it is $\mu = 0.5$ and for neutral hydrogen $\mu = 1$.

Now we assume a small shift in the density and pressure (ρ', P') from the initial balance values (ρ_0, P_0): $\rho = \rho_0 + \rho'$, $P = P_0 + P'$, $\boldsymbol{v} = \boldsymbol{v}'$. Depending on the processes, perturbations can be isothermal or adiabatic. For adiabatic changes with $\gamma = 5/3$ and isothermal with $\gamma = 1$ we can write $P/(\rho\gamma) = const = k$, so we can write $P_0 + P' = k(\rho_0 + \rho')\gamma$[1].

Linearizing the mass continuity eq. with $\nabla(\rho'\boldsymbol{v}) \to 0$ in the first approx.:

$$\frac{\partial \rho}{\partial t} + \nabla \cdot (\rho \boldsymbol{v}) = \frac{\partial}{\partial t}(\rho_0 + \rho') + \nabla \cdot \left[(\rho_0 + \rho')\boldsymbol{v}' \right] = \frac{\partial \rho'}{\partial t} + \rho_0 \nabla \cdot \boldsymbol{v}' = 0. \tag{2.20}$$

We do the same with Euler eq. to obtain:

$$\begin{aligned} (\rho_0 + \rho')\frac{\partial \boldsymbol{v}'}{\partial t} + (\rho_0 + \rho')\boldsymbol{v}' \cdot \nabla \cdot \boldsymbol{v} &= -\nabla(P_0 + P') + \boldsymbol{f} \\ \rho_0 \frac{\partial \boldsymbol{v}'}{\partial t} + \rho_0 \boldsymbol{v}' \cdot \nabla \cdot \boldsymbol{v}' &= -\nabla P_0 - \nabla P' + \boldsymbol{f}. \end{aligned} \tag{2.21}$$

Since $\nabla P_0 = \boldsymbol{f}$, and products of second and higher orders are neglected, we obtain $\rho_0 \partial_t \boldsymbol{v}' = -\nabla P'$. We obtained two equations:

$$\begin{aligned} \frac{\partial \rho'}{\partial t} + \rho_0 \nabla \cdot \boldsymbol{v}' &= 0 \\ \frac{\partial \boldsymbol{v}'}{\partial t} + \frac{1}{\rho_0}\nabla P' &= 0. \end{aligned} \tag{2.22}$$

From $P_0 + P' = k(\rho_0 + \rho')\gamma$ we see that P is a function of ρ only, so that we can write $\nabla P' = (\partial P/\partial \rho)_0 \nabla \rho'$, to the first order, where with a subscript 0 we assigned that we evaluate the derivation for the equilibrium state. The second of the equations 2.22 we can write now as:

$$\frac{\partial \boldsymbol{v}'}{\partial t} + \frac{1}{\rho_0}\left(\frac{\partial P}{\partial \rho} \right)_0 \nabla \rho' = 0. \tag{2.23}$$

[1] If $\gamma = 1$ produces a failure in the simulations, try $\gamma = 1.05$ or a similar number slightly larger than unity. Without a preset limit in the code, $\gamma = 1$ is often a problem in the isothermal case.

We act on it with the ∇ operator: $\nabla \cdot \partial_t \boldsymbol{v}' + 1/\rho(\partial\rho/\partial P)_0 \nabla^2 \rho' = 0$. We act on the first of the equations in 2.22 with $\partial/\partial t$: $\partial_t^2 \rho' + \rho_0 \nabla(\partial_t \boldsymbol{v}') = 0$. We subtract the two eqs.to obtain $\partial_t^2 \rho' = (\partial P/\partial\rho)_0 \nabla^2 \rho'$, the wave equation. With $(\partial P/\partial\rho)_0$ as a square of the sound speed c_s^2, we can write $\partial_t^2 \rho' = c_\mathrm{s}^2 \nabla^2 \rho'$.

For P' and $\boldsymbol{v}'$ we obtain the equivalent equations, so we conclude that small perturbations around the hydrostatic equilibrium positions spread with the speed of sound. Depending on the kind of perturbation, we have two possibilities, adiabatic:

$$c^\mathrm{ad} = \sqrt{\frac{5P}{3\rho}} = \sqrt{\frac{5kT}{3\mu m_\mathrm{H}}} \propto \rho^{1/3}, \text{ or isothermal } c_\mathrm{s}^\mathrm{isot} = \sqrt{\frac{P}{\rho}} = \sqrt{\frac{kT}{\mu m_\mathrm{H}}}. \tag{2.24}$$

2.2 Stationary thin disk

We obtained the equation 1.10 for the disk surface density:

$$\frac{\partial S}{\partial t} = \frac{3}{R}\frac{\partial}{\partial R}\left[\sqrt{R}\frac{\partial}{\partial R}\left(\nu S\sqrt{R}\right)\right].$$

To continue, we need the viscosity. That the disk would be "stationary" and that viscosity would work, we need that the mass accretion rate $\dot{M}$ would be slow enough. Then we can set $\partial/\partial t = 0$ and from the mass conservation we can write $\dot{M} = 2\pi R S(-v_r)$ and from the angular momentum conservation we have $RSv_r R^2\Omega = (J(R,t) + C)/(2\pi))$, with $C = const.$ related to the angular momentum rate of the accreted matter. Star must rotate slower than the breakup rotation at the equator, so when approaching closer to the star, there is a region in the disk where the disk co-rotates with the star. Even closer to the star, our approximation breaks-here starts the discussion and departure from the simple estimates.

We had $J = J(R,t)$, and with $R\partial\Omega/\partial R = A$ it was $J(R) = 2\pi R\nu SAR$, where νSA is a viscous force per unit angle. After integration:

$$-\nu S\frac{\partial\Omega}{\partial R} = S(-v_r\Omega) + \frac{C}{2\pi R^3}. \tag{2.25}$$

Inside a ring at $R_A + b$, the rotation of the disk approaches Keplerian, reaches $\partial\Omega/\partial R = 0$, and increases until it reaches $R \sim R_A$. We can write:

$$\Omega(R_A + b) = \sqrt{\frac{GM}{R_A^3}}\left[1 + \mathcal{O}\left(\frac{b}{R_A}\right)\right]. \tag{2.26}$$

Closer than R_A The thin disk approximation is not valid anymore. To find C we insert $R = R_A + b$ and evaluate $C = 2\pi R_A 3 S v_r \Omega(R_A + b)|R_A + b$ (now $\Omega()$, not multiplying!), which gives, after inserting mass accretion rate $\dot{M}$ and $\Omega(R_A + b)$, that $C = -\dot{M}\sqrt{GMR_A}$, exact to order $\mathcal{O}(b/R_A)$. We insert it to eq. 2.25 to obtain:

$$\nu S = \frac{\dot{M}}{3\pi}\left[1 - \sqrt{\frac{R_A}{R}}\right]. \tag{2.27}$$

Loss of energy because of viscosity is

$$D(R) = \frac{g}{4\pi}\frac{\partial\Omega}{\partial R} = \frac{1}{2}(\nu S)\left(R\frac{\partial\Omega}{\partial R}\right)^2 \tag{2.28}$$

which is $D(R) = g/(4pi)\partial\Omega/\partial R$ per unit disk surface (g is the gravitational acceleration). Inserted back to eq. 2.25 it gives that $D(R)$ is independent of viscosity:

$$D(R) = \frac{3GM\dot{M}}{8\pi R^3}\left[1 - \sqrt{\frac{R_A}{R}}\right]. \tag{2.29}$$

Now we can estimate the luminosity of a disk between R_1 and R_2 (factor 2 is for 2 disk sides):

$$L(R_1, R_2) = 2\int_{R_1}^{R_2} D(R) 2\pi R dR = \frac{3}{2} GM\dot{M} \int_{R_1}^{R_2} \left[1 - \sqrt{\frac{R_A}{R}}\right] \frac{dR}{R^2}. \tag{2.30}$$

If we substitute $x = R/R_A$, we obtain

$$L(R_1, R_2) = 2\int_{R_1}^{R_2} D(R) 2\pi R dR = \\ \frac{3}{2} GM\dot{M} \left[\frac{1}{R_1}\left(1 - \frac{2}{3}\sqrt{\frac{R_A}{R_1}}\right) - \frac{1}{R_2}\left(1 - \frac{2}{3}\sqrt{\frac{R_A}{R_2}}\right)\right]. \tag{2.31}$$

For $R = R_1$ and $R_2 \to \infty$ we obtain the complete disk luminosity:

$$L_{disk} = \frac{GM\dot{M}}{2R_A} = \frac{1}{2} L_{accr}, \tag{2.32}$$

where we defined $L_{accr} = \Delta E_{accr}/\Delta t = GM\dot{M}/R_A$. This means that half of the energy is radiated from the disk, and half is released very close to the central star, which takes the same amount like the whole disk! (which has a much, much larger surface).

This was derived for a radial direction, is it all consistent with the vertical direction? In the vertical, z direction, there is mainly no flow, we have the hydrostatic equilibrium:

$$\frac{1}{\rho}\frac{\partial P}{\partial z} = \frac{\partial}{\partial z}\left[\frac{GM}{\sqrt{R^2 + z^2}}\right] \tag{2.33}$$

which we get from the vertical component of the Euler eq. 2.7, neglecting all the terms with velocities. For the thin disk $z \ll R$ we have:

$$\frac{1}{\rho}\frac{\partial P}{\partial z} = -\frac{GMz}{R^3}. \tag{2.34}$$

Since $H || z$ we can write $\partial P/\partial z \sim P/H$ and $z \sim H$, and condition for a thin disk becomes $H \ll R$. For $P \propto \rho c_{\rm s}^2$ we have $H \simeq c_{\rm s} R^4 \sqrt{R/GM}$, which means that it has to be $c_{\rm s} \ll \sqrt{GM/R}$ and there is an additional condition for a thin disk: local Keplerian speed must be *highly supersonic*. Only with this satisfied, the approximation of thin disk can be used. This is a strong condition for the inner workings of a disk, and tells us that the local orbiting speed will be close to the Keplerian speed.

The radial component of the Euler eq.is:

$$v_r \frac{\partial v_r}{\partial R} - \frac{v_\varphi}{R} + \frac{1}{\rho}\frac{\partial P}{\partial R} + \frac{GM}{R^2} = 0. \tag{2.35}$$

If we neglect the pressure term, because of $c_{\rm s} \ll \sqrt{GM/R}$, we have $\rho^{-1}\partial P/\partial R \sim c_{\rm s}^2/R$ in comparison to a larger gravitational term GM/R^2, with $\dot{M} = 4\pi r \rho(-v_r)$ which we know from before, and eq. 2.25 we have

$$v_r = -\frac{3\nu}{2R}\left(1 - \sqrt{\frac{R_A}{R}}\right)^{-1}. \tag{2.36}$$

Now we are slowly shifting to the [SS73] main assumption: for any reasonable viscosity, the radial velocity vr is highly subsonic, while orbital velocity is highly supersonic and approximately Keplerian: with $\nu \propto C_{\rm s} H$ we have $v_r \propto \nu/R \sim c_{\rm s} H/R \ll c_{\rm s}$ Now we have all the equations for the disk structure.

2.3 Shakura & Sunyaev viscous alpha disk

Now we are in a better position to discuss the Shakura & Sunyaev (1973) [SS73] paper[2], which is one of the most cited papers on accretion disks[3]. It got a reprint in A&A in 2009, and a review by Andrew King, which best describes its importance. It is an epithomy of a seminal paper.

With the thin disk approximation, we can compute the structure of the disk. In practice, we are solving the 1D with only a radial dependence, as we decoupled it from the vertical, z-dependence, which is essentially written as a hydrostatic equilibrium and energy transport. In the radial direction, the disk structure enters only in the local energy dissipation rate $D(R)$. From the hydrostatic eq. 2.34 for isothermal structure we obtain the solution $\rho(R,z) = \rho_{\rm c}(R)\exp\left(-z^2/2H^2\right)$, where $\rho_{\rm c}$ stands for the density at $z=0$.

The central density of the disk we can approximate as $\rho = S/H$, where $H = \rho c_{\rm s}/v_\varphi$ and $c_{\rm s}^2 = P/\rho$, where $P = P_{\rm g} + P_{\rm rad} = \rho k T_{\rm c}/(\mu m_{\rm H}) + 4\sigma T_{\rm c}^4/(3c)$ is a sum of gas and radiation pressure, with an assumption $T(T,z) \sim T_{\rm c}(R,0)$. The central temperature $T_{\rm c}$ is determined by the relation between the vertical energy flux and the energy dissipation because of viscosity. Locally, using the thin disk approximation, we now have the vertical temperature gradient, so that for $z = const.$ surface we have radiated energy flux

$$F(z) = -\frac{16\sigma T^3}{3\kappa_{\rm R}\rho}\frac{\partial T}{\partial z}, \tag{2.37}$$

where $\kappa_{\rm R}$ is the Rosseland mean opacity. We assumed the optically thick disk, with $\tau = \rho H \kappa_{\rm R} = S\kappa_{\rm R} \gg 1$, so that the radiation is locally very close to the black body radiation. In the case with $\tau \leq 1$ radiation could directly exit the disk, and the equation for $F(z)$ above would not be valid any more. For the energetic balance it must be $F(H) - F(0) = D(R)$, so that $F(z) \sim 4\sigma T^4(z)/(3\tau)$ which, with $T_{\rm c}^4 \gg T^4(H)$ gives $4\sigma T_{\rm c}^4(z)/(3\tau) = D(R)$. For the full set of equations we need the $\kappa_{\rm R} = \kappa_{\rm R}(\rho, T_{\rm c})$ relation, and an expression for ν and its relation to S and $\dot{M}$. This all amounts to 8 equations for ρ, S, H, $T_{\rm c}$, $c_{\rm s}$, P, τ, ν in dependence of R, M and $\dot{M}$, with some parameter in the viscosity, which are describing the thin disk model:

$$\begin{aligned}
&(D1)\ \rho = \frac{S}{H},\ (D2)\ H = \frac{c_{\rm s}R^{3/2}}{\sqrt{GM}},\ (D3)\ c_{\rm s} = \frac{P}{\rho}, (D4)\ P = \frac{\rho k T_{\rm c}}{\mu m_{\rm H}} + \frac{4\sigma T_{\rm c}^4}{3c},\\
&(D5)\ \frac{4\sigma T_{\rm c}^4}{3\tau} = \frac{3GM\dot{M}}{8\pi R^3}\left[1-\sqrt{\frac{R_A}{R}}\right],\ (D6)\tau = S\kappa_{\rm R}(\rho,T_{\rm c}) = \tau(S,\rho,T_{\rm c}),\\
&(D7)\ \nu S = \frac{\dot{M}}{3\pi}\left[1-\sqrt{\frac{R_A}{R}}\right],\ (D8)\ \nu = \nu(\rho,T_{\rm c},S,\alpha,\dots).
\end{aligned} \tag{2.38}$$

With "alpha viscosity" parameterization $\nu = \alpha c_{\rm s} H$, [SS73] gave the first solution. They used the Kramers' law[4] $\kappa_{\rm R} = 5\times 10^{24}\rho T_{\rm c}^{-7/2}\ cm^2/g$ and neglected the radiation pressure in eq. D4 of 2.38. Now the system of 8 equations D1-D8 can be solved. I give steps (from the "Accretion power..."- book [FKR02] for easier navigating through the solution: First we simplify $f^4 = \left[1-(R_A/R)^{1/2}\right]$ and write whole r.h.s. of eq. D5 as equal to D. Now with eq. D6, $\kappa_{\rm R}$ and eq. D2 we can write eq. D5 as $4\sigma T^4/(3\tau) = D = 4\sigma T^{15/2}/(3\cdot 5\cdot 10^{24}\rho S) = (\rho = S/H) = 4\sigma H T^{15/2}/(15\cdot 10^{24}S^2) = H = c_{\rm s}R^{3/2}/\sqrt{GM}$ and from eqs. D3 and D4 (without $P_{\rm rad}$ pressure term) write

$$H = R^{3/2}\sqrt{T}\left[k_{\rm B}/(GM\mu m_{\rm p})\right]^{1/2} = 4\sigma R^{3/2}T^8\left[k_{\rm B}/(GM\mu m_{\rm p})\right]^{1/2}/(15\cdot 10^{24}S^2), \tag{2.39}$$

[2]Usually cited before Shakura & Sunyaev disk is Lynden-Bell [Lyn69] discussion of the origin of emission from galactic nuclei - "old quasars", where *Schwarzschild mouth* was still the term for the event horizon.

[3]Citation count in the NASA ADS was at 10657 at noon Sunday 27.02.2022, 10909 half year later, at 27.08.2022, so it is still steadily accreting citations.

[4]Beware that in many publications the value is given wrongly as 6.6×10^{22}.

and from that obtain $T^8 = 15 \cdot 10^{24} S^2 D \left[k_{\rm B}/(GM\mu m_{\rm p})\right]^{1/2} /(4\sigma R^{3/2})$. We insert D back as the r.h.s of eq. D5 and use eqs. D7 and D8 (where $\nu = \alpha c_{\rm s} H$ comes finally into use), to write the solution-I give the detailed derivation of solutions below in the text, this is usually not shown in literature. Now we can write v_r from the equation we obtained at the end of the previous section, $v_r \propto \nu/R \sim c_{\rm s} H/R \ll c_{\rm s}$.

2.3.1 Surface density

eq. D5 with eq. D6 and $\kappa_R = 5 \cdot 10^{24} \rho T^{-7/2}$ gives

$$\frac{4\sigma T^4}{3S5 \cdot 10^{24} \rho T^{-7/2}} = \frac{3GM\dot{M}}{8\pi R^3}\left(1 - \sqrt{\frac{R_A}{R}}\right) \tag{2.40}$$

Using eqs. D1 and D2

$$\rho = \frac{S}{H} = \frac{S}{c_s}\sqrt{\frac{GM}{R^3}} \tag{2.41}$$

By substituting $c_s = \sqrt{\frac{P}{\rho}} = \sqrt{\frac{kT}{\mu m_H}}$ from eq. D3 and eq. D4, we obtain,

$$\rho = S\sqrt{\frac{GM}{R^3}\frac{\mu m_H}{kT}} \tag{2.42}$$

Going back to eq. 2.40:

$$\frac{4\sigma T^4}{3S5 \cdot 10^{24} S\sqrt{\frac{GM}{R^3}\frac{\mu m_H}{kT}} T^{-7/2}} = \frac{3GM\dot{M}}{8\pi R^3}\left(1 - \sqrt{\frac{R_A}{R}}\right) \tag{2.43}$$

and we solve for T:

$$T^8 = \frac{45 \cdot 10^{24}}{32\pi\sigma} S^2 \left(\frac{GM}{R^3}\right)^{3/2} \dot{M}\sqrt{\frac{\mu m_H}{k}}\left(1 - \sqrt{\frac{R_A}{R}}\right) \tag{2.44}$$

eq. D8 in eq. D7 $\alpha c_s H S = \frac{\dot{M}}{3\pi}\left(1 - \sqrt{\frac{R_A}{R}}\right)$, since

$$\frac{\alpha c_s^2}{\sqrt{\frac{GM}{R^3}}} S = \frac{\dot{M}}{3\pi}\left(1 - \sqrt{\frac{R_A}{R}}\right) \Rightarrow \text{(from eqs. D3 and D4)} \Rightarrow$$

$$\alpha \frac{kT}{\mu m_H} \frac{S}{\sqrt{\frac{GM}{R^3}}} = \frac{\dot{M}}{3\pi}\left(1 - \sqrt{\frac{R_A}{R}}\right) \Rightarrow$$

$$T = \frac{\mu m_H}{kS\alpha}\frac{\dot{M}}{3\pi}\left(1 - \sqrt{\frac{R_A}{R}}\right)$$

Now we put it into eq. 2.44,

$$\left[\frac{\mu m_H}{kS\alpha}\frac{\dot{M}}{3\pi}\left(1 - \sqrt{\frac{R_A}{R}}\right)\right]^8 = \frac{45 \cdot 10^{24}}{32\pi\sigma} S^2 \left(\frac{GM}{R^3}\right)^{3/2} \dot{M}\sqrt{\frac{\mu m_H}{k}}\left(1 - \sqrt{\frac{R_A}{R}}\right),$$

and we solve for S.

$$S^{10} = \left(\frac{\mu m_H}{k}\right)^{15/2} \frac{\dot{M}^7 32\pi\sigma}{45\cdot 10^{24}} \frac{1}{(3\pi\alpha)^8} \left(1-\sqrt{\frac{R_A}{R}}\right)^7 \left(\frac{R^3}{GM}\right)^{3/2} \Rightarrow$$

$$S = \left(\frac{\mu m_H}{k}\right)^{3/4} \left(\frac{32\pi\sigma}{45\cdot 10^{24}}\right)^{1/10} \frac{\alpha^{-4/5}\dot{M}^{7/10}}{(3\pi)^{4/5}} \left(\frac{R^3}{GM}\right)^{3/20} \left(1-\sqrt{\frac{R_A}{R}}\right)^{7/10} \tag{2.45}$$

2.3.2 Disk height

$$H = c_s\sqrt{\frac{R^3}{GM}} = \sqrt{\frac{kT}{\mu m_H}\frac{R^3}{GM}}$$

$$H^{16} = \left(\frac{k}{\mu m_H}\frac{R^3}{GM}\right)^8 T^8 = \left(\frac{k}{\mu m_H}\frac{R^3}{GM}\right)^8 \frac{45\cdot 10^{24}}{32\pi\sigma} S^2 \left(\frac{GM}{R^3}\right)^{3/2} \dot{M}\sqrt{\frac{\mu m_H}{k}} \left(1-\sqrt{\frac{R_A}{R}}\right)$$

$$H^8 = \left(\frac{k}{\mu m_H}\frac{R^3}{GM}\right)^4 \left(\frac{45\cdot 10^{24}}{32\pi\sigma}\right)^{1/2} S \left(\frac{GM}{R^3}\right)^{3/4} \dot{M}^{1/2} \left(\frac{\mu m_H}{k}\right)^{1/4} \left(1-\sqrt{\frac{R_A}{R}}\right)^{1/2} =$$

$$= \left(\frac{k}{\mu m_H}\right)^{15/4} \left(\frac{R^3}{GM}\right)^{13/4} \dot{M}^{1/2} \left(\frac{45\cdot 10^{24}}{32\pi\sigma}\right)^{1/2} \left(1-\sqrt{\frac{R_A}{R}}\right)^{1/2} S =$$

$$= \left(\frac{k}{\mu m_H}\right)^{15/4} \left(\frac{R^3}{GM}\right)^{13/4} \dot{M}^{1/2} \left(\frac{45\cdot 10^{24}}{32\pi\sigma}\right)^{1/2} \left(1-\sqrt{\frac{R_A}{R}}\right)^{1/2} \cdot$$

$$\cdot \left(\frac{\mu m_H}{k}\right)^{3/4} \left(\frac{32\pi\sigma}{45\cdot 10^{24}}\right)^{1/10} \frac{\alpha^{-4/5}}{(3\pi)^{4/5}} \left(\frac{GM}{R^3}\right)^{-3/20} \left(1-\sqrt{\frac{R_A}{R}}\right)^{7/10} \dot{M}^{7/10} =$$

$$= \left(\frac{k}{\mu m_H}\right)^3 \left(\frac{R^3}{GM}\right)^{17/5} \dot{M}^{6/5} \left(\frac{32\pi\sigma}{45\cdot 10^{24}}\right)^{-2/5} \left(1-\sqrt{\frac{R_A}{R}}\right)^{6/5} \frac{\alpha^{-4/5}}{(3\pi)^{4/5}}$$

$$H = \left(\frac{k}{\mu m_H}\right)^{3/8} \left(\frac{R^3}{GM}\right)^{17/40} \dot{M}^{3/20} \left(\frac{32\pi\sigma}{45\cdot 10^{24}}\right)^{-1/20} \left(1-\sqrt{\frac{R_A}{R}}\right)^{3/20} \frac{\alpha^{-1/10}}{(3\pi)^{1/10}}. \tag{2.46}$$

2.3.3 Mass density

$$\rho = \frac{S}{H} = \frac{\left(\frac{\mu m_H}{k}\right)^{3/4} \left(\frac{32\pi\sigma}{45\cdot 10^{24}}\right)^{1/10} \frac{\alpha^{-4/5}\dot{M}^{7/10}}{(3\pi)^{4/5}} \left(\frac{R^3}{GM}\right)^{3/20} \left(1-\sqrt{\frac{R_A}{R}}\right)^{7/10}}{\left(\frac{k}{\mu m_H}\right)^{3/8} \left(\frac{R^3}{GM}\right)^{17/40} \dot{M}^{3/20} \left(\frac{32\pi\sigma}{45\cdot 10^{24}}\right)^{-1/20} \left(1-\sqrt{\frac{R_A}{R}}\right)^{3/20} \frac{\alpha^{-1/10}}{(3\pi)^{1/10}}} =$$

$$= \left(\frac{\mu m_H}{k}\right)^{3/8} \left(\frac{R^3}{GM}\right)^{17/40} \dot{M}^{3/20} \left(\frac{32\pi\sigma}{45\cdot 10^{24}}\right)^{-1/20} \left(1-\sqrt{\frac{R_A}{R}}\right)^{11/20} \frac{\alpha^{-7/10}}{(3\pi)^{7/10}}. \tag{2.47}$$

2.3.4 Temperature

From 2.44 we have

$$T = \left(\frac{45\cdot 10^{24}}{32\pi\sigma}\right)^{1/8} S^{1/4}\left(\frac{GM}{R^3}\right)^{3/16}\dot{M}^{1/8}\left(\frac{\mu m_H}{k}\right)^{1/16}\left(1-\sqrt{\frac{R_A}{R}}\right)^{1/8} =$$
$$= \left(\frac{45\cdot 10^{24}}{32\pi\sigma}\right)^{1/10}\left(\frac{GM}{R^3}\right)^{3/20}\left(\frac{\mu m_H}{k}\right)^{1/4}\dot{M}^{3/10}\frac{\alpha^{-1/5}}{(3\pi)^{1/5}}\left(1-\sqrt{\frac{R_A}{R}}\right)^{3/10}. \tag{2.48}$$

2.3.5 Optical depth

From eq. D6 we have, inserting ρ and T:

$$\tau = 5\times 10^{24} S\rho T^{-7/2} =$$
$$= 5\times 10^{24}\left(\frac{\mu m_H}{k}\right)^{1/4}\left(\frac{45\cdot 10^{24}}{32\pi\sigma}\right)^{-2/5}\frac{\dot{M}^{-1/5}\alpha^{-4/5}}{(3\pi)^{4/5}}\left(\frac{GM}{R^3}\right)^{11/10}\left(1-\sqrt{\frac{R_A}{R}}\right)^{1/5}. \tag{2.49}$$

2.3.6 Viscosity

From eq. D8

$$\nu = \alpha c_s H = \alpha H^2\sqrt{\frac{GM}{R^3}} =$$
$$= \left(\frac{k}{\mu m_H}\right)^{3/4}\left(\frac{R^3}{GM}\right)^{7/20}\dot{M}^{3/10}\left(\frac{32\pi\sigma}{45\cdot 10^{24}}\right)^{-1/10}\left(1-\sqrt{\frac{R_A}{R}}\right)^{3/10}\frac{\alpha^{4/5}}{(3\pi)^{1/5}}. \tag{2.50}$$

2.3.7 Velocity

From eq. 2.36 we now can write the radial velocity in the disk:

$$v_r = -\frac{3\nu}{2R}\left(1-\sqrt{\frac{R_A}{R}}\right)^{-1} =$$
$$= -\frac{3\dot{M}^{3/10}}{2R}\left(\frac{k}{\mu m_H}\right)^{3/4}\left(\frac{R^3}{GM}\right)^{7/20}\left(\frac{32\pi\sigma}{45\cdot 10^{24}}\right)^{-1/10}\left(1-\sqrt{\frac{R_A}{R}}\right)^{-7/10}. \tag{2.51}$$

In the literature, we usually find the solutions above written with $R_{10} = R/10^{10}$cm, $M_1 = M/M_\odot$, $\dot{M}_{16} = \dot{M}/(10^{16} g s^{-1})$, $\mu = 0.615$, $f = (1-\sqrt{R/R_A})^{1/4}$ as:

$$\begin{aligned}
S &= 5.2\alpha^{-4/5}\dot{M}_{16}^{7/10}M_1^{1/4}R_{10}^{-3/4}f^{11/5}\ gcm^{-2},\\
H &= 1.7\times 10^8\alpha^{-1/10}\dot{M}_{16}^{3/20}M_1^{-3/8}R_{10}^{9/8}f^{3/5}\ cm,\\
\rho &= 3.1\times 10^{-8}\alpha^{-7/10}\dot{M}_{16}^{11/20}M_1^{5/8}R_{10}^{-15/8}f^{11/5}\ gcm^{-3},\\
T &= 1.4\times 10^4\alpha^{-1/5}\dot{M}_{16}^{3/10}M_1^{1/4}R_{10}^{-3/4}f^{6/5}\ K,\\
\tau &= 190\alpha^{-4/5}\dot{M}_{16}^{1/5}f^{4/5},\\
\nu &= 1.8\times 10^{14}\alpha^{4/5}\dot{M}_{16}^{3/10}M_1^{-1/4}R_{10}^{3/4}f^{6/5}\ cm^2 s^{-1},\\
v_r &= 2.7\times 10^4\alpha^{4/5}\dot{M}_{16}^{3/10}M_1^{-1/4}R_{10}^{-1/4}f^{-14/5}\ cms^{-1}.
\end{aligned} \tag{2.52}$$

It is important that α is nowhere coming with large power, so that any error because of our not knowing it, is less.

The Kramers' law for $\kappa_{\rm R}$ is critical, because when it is not holding any more, our approximation breaks down, but until it holds, disk can extend far in R, of the order of Roche boundary of the more massive star. Mass in the disk is

$$M_{\rm disk} = 2\pi \int_{R_A}^{R_{\rm external}} SRdR \leq 10^{-10} M_\odot \alpha^{-4/5} \dot{M}_{16}^{7/10}, \tag{2.53}$$

which is even in the very large disks negligible in comparison with the central object. This justifies the neglect of self-gravity of a disk, which is valid until $\rho \ll M/R^3$. Only for a very small α, of the order of 10^{-10}, this would not be fulfilled. The disk thickness in z-direction means that each element of the disc surface radiates as a black body with a temperature $T(R)$ given by equating the dissipation rate $D(R)$ per unit face area to the black body flux: $\sigma T^4 = D(R)$. If we insert D from above,

$$T(R) = \left[\frac{3GM\dot{M}}{8\pi R^3\sigma}\left(1-\sqrt{\frac{R_\star}{R}}\right)\right]^{1/4}. \tag{2.54}$$

For $R \gg R_\star$, $T = T_\star (R/R_\star)^{-3/4}$, where

$$T_\star = \frac{3GM\dot{M}}{8\pi R_\star^3\sigma}^{1/4}, \tag{2.55}$$

which gives $4.1\times 10^4 \dot{M}_{16}^{1/4} m_1^{1/4} R_9^{-3/4}$ K and $1.3\times 10^7 \dot{M}_{17}^{1/4} m_1^{1/4} R_6^{-3/4}$ K with $R_9 = R_\star/10^9$ cm etc. for a disk around white dwarf and $R_6 = R_\star/10^6$ cm, respectively, in the case of neutron star[5].

The low power of α in the equations is good for usefulness of α as a parameter, but it also means we cannot expect to learn the typical size of α by direct comparison of steady-state disc theory with observations. This is something what is troubling disk astrophysics until today. No free lunch!

A good thing is that for $\alpha \leq 1$ we obtained solutions, which are not too much off the models from observational data. Where we expect the assumptions (Kramers' opacity and the neglect of radiation pressure) to break down? We have $\kappa_{\rm R} = \tau/S = 36\dot{M}_{16}^{-1/2} m_1^{1/4} R_{10}^{3/4} f^{-2}$ in $\dot{M}_{16}^{2/3} m_1^{1/3} f^{8/3}$ cm. This is smaller than the radius of a white dwarf for any reasonable $\dot{M}$, so for the accretion discs in cataclysmic variables we expect Kramers' opacity to dominate in most of the disc.

In a reasonable range we can rely on the results for the physical regimes in steady α-discs around compact objects. If the disk is concave, then the central, hot regions, could irradiate the more distant, colder parts of the disk with hard radiation, and the picture complicates-this would show in observations. Similar would be for a warped disk, where a non-central force of photons scattered from the disk surface would produce torque on the disk.

If the disk is concave, then the central, hot regions, could irradiate the more distant, colder parts of the disk with hard radiation, and the picture complicates-this would show in observations. E.g. in low-mass X-ray binaries the disk is probably heated by irradiation by the central accretion source. If the accretor is a luminous star, we can have a similar effect.

2.4 Working of MRI in the disk

Alpha viscosity does not give us predictive power. Since $\partial/\partial R(R^2\Omega) = 0$ (Rayleigh criterion, stability against axisymmetric perturbations) and $\partial\Omega/\partial R) < 0$. Most potential mechanisms are sensitive to the angular momentum gradient, so they work in such a way that they are bringing angular momentum INWARDS. We need a mechanism sensitive to Ω.

[5] Note that now it is $R_A = R_\star$.

If not alpha viscosity, then what? How the MRI works? Balbus-Hawley (1992) (magnetorotational, MRI) instability. If we imagine a straight magnetic field B line threading a rotating disc, magnetic tension tries to straighten line, there is imbalance between gravity and rotation which bends the magnetic field line.

Vertical field line perturbed outwards, rotates faster than surroundings, so centrifugal force is larger than gravity, so that kink increases. Line connects fast-moving (inner) matter with slower (outer) matter, and speeds latter up: this produces outwards angular momentum transport!

For a too large magnetic field, instability is suppressed. Distorted fieldline stretched in the azimuthal direction by differential rotation, strength grows, pressure balance between flux tube and surroundings requires $B^2/8\pi + P_{gas,in} = P_{gas,out}$, so that gas pressure (and density) are lower inside tube; buoyant (Parker) instability works, and Flux tube rises above the disk, creating another vertical field, which closes the cycle, which can transport the angular momentum – this was shown to work in numerical simulations.

2.5 Self-gravity in the disk

Another effect which will change the picture is when the disk becomes larger. E.g. the size of AGN disk is set by self-gravity: vertical component of gravity from central mass is $\sim GMH/R^3$ and from self-gravity $\sim G\rho H^3/H^2 = G\rho H$. Thus self-gravity takes over where $\rho \sim M/R^3$ or $M_{disk} \sim R^2 H\rho \sim HM/R$. Outside of this region, disk breaks-up into stars.

Chapter 3

General accretion disk solutions

3.1 Urpin's and Regev's vertically averaged solutions

We mentioned before the z-averaged solutions. Assumptions in Urpin (1984) [Urp84] are all as in SS73 solution. He discusses the obtained solutions in the different regions in the disk, similar to SS73. It is interesting that in his approach he first obtained the accretion flow in the disk having two directions: near the disk mid-plane it is away from the central object[1], and higher in the disk, it is towards the central object. Still, in his solution, mass accretion rate towards the star exceeds the outward flow by a factor 4 or 5, depending on the considered zone.

In Regev (1983) [Reg83], a solution by expansion on a small parameter of H/R is proposed. On this, later similar solutions are developed. To better understand the subsequent development, we briefly discuss his solution.

Boundary layer between the inner disk radius and stellar surface is important-there $\Omega_{\rm K}$ of the infalling material changes to $\Omega_\star$ in a very thin layer, compared to the disk extension in radius. As we obtained in the previous chapter, up to a half of the accretion luminosity is generated in this thin layer.

In SS73, Pringle (1981) [Pri81] and similar, $d\Omega/dr = 0$ is used at $r = r_\star$ boundary. Solutions by Regev, applied to a disk around a white dwarf relate to region (c) in SS73. He searches for steady, axisymmetric solutions, with $\partial/\partial t = \partial/\partial\varphi = 0$, viscosity is present (only $r-\varphi$ component of the viscous stress tensor, the rest of it is neglected), the disk is optically thick, with radiation transfer treated in the diffusion approximation.

He solves the usual equations: momentum eq. in r and z directions (in cylindrical coords), angular momentum (in radial direction), mass continuity and energy equations. He prescribes the radiative energy fluxes in r and z directions assuming the optically thick disk, with radiation transfer treated in the diffusion approximation

We need to supply the equation of state for P and opacity κ_R. The constant mass flux through the disk is another requirement, which is a constraint for the solution: $-2\pi r \int_\infty^\infty \rho u dz = \dot{M} = const.$

We will not follow Regev solution, because we will improve on it with KK solution. We only mention that he used the "method of matched asymptotic expansions"[2].

The ideal gas eq.is assumed, the radiative term neglected, opacity for free-free transitions is assumed, in the main solution and also in the boundary layer. Viscosity in the boundary layer is assumed as $\nu BL = KV{\rm turb}\Lambda$, with K and $V{\rm turb}$ constant and Λ being a characteristic length scale in the boundary layer. In the non-dimensional units it is

$$\nu_{\rm BL} = \frac{K}{\alpha}\frac{v_{\rm turb}}{\tilde{v}_s}\frac{\Lambda}{\tilde{H}}. \tag{3.1}$$

[1] We call it backflow in the later text.

[2] Regev refers to it as "Bender & Orszag (1978, chapter 9) solution for differential eqs. which exhibit a boundary layer structure". I usually refer to it as performing a Taylor expansion in a small parameter ϵ, as this is to what we resort at the end.

Regev uses the "matched" part of the solution at the boundaries to ensure the physicality of solutions. An "outer" expansion at $r \neq 1,\ \epsilon \to 0$ is constructed and matched to the inner expansion, valid in the disk. Similar is done for the inner region, in the case when star is fast rotating, near the breakup velocity, he assumes $\Omega_\star = \epsilon^{1/2}\Omega_{\mathrm{K},\star}$. This is different from KK solution, where this constraint is relaxed.

Regev's is another z-averaged solution, only more involved than Urpin's. The obtained equations need to be solved numerically, in difference to KK solution, which we will derive analytically.

3.2 Kluźniak-Kita 3D global solution

The work in Kluźniak & Kita (2000) [KK00, hereafter KK00] paper, which exists only in arXiv version[3], is actually a PhD thesis of David Kita from 1995 at Madison University, USA [Kit95][4]. It is a general solution obtained similarly to Regev's, but without assumptions he used at the inner disk radius. It is a 3D, axisymmetric, purely HD solution.

We will go through the process of deriving asymptotic matched solutions in, again sometimes painful, detail. It is a very instructive example, and it could be of use for other similar work.

Motivation of KK00 paper is to find the solutions which would show that the backflow, which appeared also in other solutions except Urpin and Regev, is not of a thermal origin. Urpin included thermal effects but made the simplification of zero net angular momentum flow in the disk (equivalently, his self-similar solution is valid asymptotically for large radii). KK chose the opposite route—neglect thermal effects, but include the inner boundary condition. They were able to find a global solution. They show how the backflow is fed by the inflowing fluid. An interesting note: Narayan & Yi (1995) [NY95] went beyond the one-dimensional solutions by numerically constructing axisymmetric ADF solutions which factorize the three-dimensional equations, i.e., solutions of the type $f(r,\theta) = R(r)\Theta(\theta)$. Solutions in KK00 are not factorizable.

Not to repeat the lengthy derivations twice, we will do the magnetic version, and outline the HD solutions by setting B=0[5]

Since the set of HD equations is closed, the purely HD solutions can be obtained. For the magnetic case it is not the case, and only some general conditions can be obtained. With help of numerical simulations I verified both the HD and non-ideal MHD solution, and found they are in great agreement. I will illustrate it later.

We search for the quasi-stationary state solutions, assuming that all the heating is radiated away from the disk. This is why the dissipative viscous and resistive terms are not present in the energy equation, nor are the cooling terms. We still solve the equations in the non-ideal MHD regime, because of the viscous terms in the momentum equation, and the Ohmic resistive term in the induction equation. We are solving viscous

[3] KK00 paper in arXiv is with figures given at the end, I rearranged it and made a more handy version with figures positioned in their places in the text. It is downloadable from the webpage: http://web.tiara.sinica.edu.tw/ miki/PostPrez/KK00mikiversion.pdf

[4] Thesis is not available online, it is only in hard copy in the library in USA and an example in CAMK, Warsaw-but arXiv paper is very similar to the Thesis, all the formalism is copied in the paper.

[5] It is interesting that both are non-published work, present only in arXiv, referees did not appreciate the contributions, yet. KK00 paper has a decent following and it will stay in arXiv domain. The more recent magnetic generalization presented here is still in push for the peer-reviewed publication.

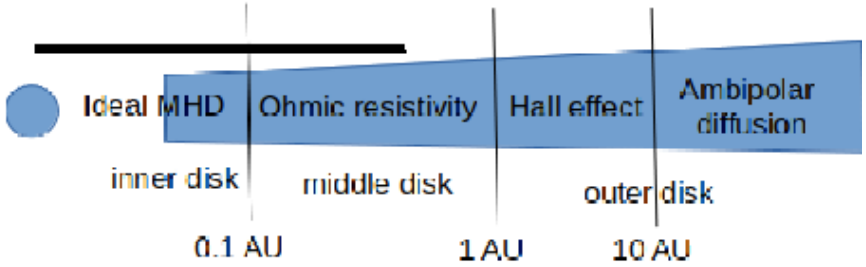

Figure 3.1: Illustration of the reach of the inner, middle and outer disk regions in the case of Young Stellar Objects. In the innermost disk region the disk is in the ideal MHD regime. Further away from the star, in the middle disk region, the Ohmic resistivity adds to the viscous dissipation. In the outer disk, which we do not analyze here, other resistive terms prevail in the induction equation. Radial extension of the physical domain in our simulations is indicated with the horizontal thick black solid line. Figure is taken from [ČPK18].

and resistive MHD equations (in the cgs units):

$$\frac{\partial \rho}{\partial t} + \nabla \cdot (\rho \mathbf{v}) = 0 \tag{3.2}$$

$$\nabla \cdot \mathbf{B} = 0 \tag{3.3}$$

$$\frac{\partial \rho \mathbf{v}}{\partial t} + \nabla \cdot \left[\rho \mathbf{v}\mathbf{v} + \left(P + \frac{B^2}{8\pi} \right) \tilde{I} - \frac{\mathbf{B}\mathbf{B}}{4\pi} - \tilde{\tau} \right] = \rho \mathbf{g} \tag{3.4}$$

$$\frac{\partial E}{\partial t} + \nabla \cdot \left[\left(E + P + \frac{B^2}{8\pi} \right) \mathbf{v} - \frac{(\mathbf{v} \cdot \mathbf{B})\mathbf{B}}{4\pi} \right] = \rho \mathbf{g} \cdot \mathbf{v} \tag{3.5}$$

$$\frac{\partial \mathbf{B}}{\partial t} + \nabla \times (\mathbf{B} \times \mathbf{v} + \eta_{\mathrm{m}} \mathbf{J}) = 0, \tag{3.6}$$

with ρ, P, $\mathbf{v}$, $\mathbf{B}$ and η_{m} being the density, pressure, velocity, magnetic field and the Ohmic resistivity, respectively. The acceleration of gravity is $\mathbf{g} = -\nabla \Phi_{\mathrm{g}}$, and the gravitational potential of the star with mass $M_\star$ is $\Phi_{\mathrm{g}} = -GM_\star/R$. The total energy density $E = P/(\gamma - 1) + \rho v^2/2$ and the electric current are given by Ampere's law $\mathbf{J} = \nabla \times \mathbf{B}/(4\pi)$. An ideal gas is assumed, with the plasma adiabatic index $\gamma = 5/3$, or a polytropic index $n = 3/2$. The unit tensor and the viscous stress tensor, respectively are represented by the terms $\tilde{I}$ and $\tilde{\tau}$.

Normalized units are used, so that we could compare the magnitude of the different terms in the equations. All the variables are written in the Taylor expansion, with the coefficient of expansion given by the characteristic ratio of disk height to the radius, $\epsilon = H/R << 1$. For a variable X we have then $X = X_0 + \epsilon X_1 + \epsilon^2 X_2 + \epsilon^3 X_3 + \ldots$ and we can compare the terms of the same order in ϵ for each variable.

In the case of a viscous, purely HD disk ($B = 0$), the equations can be solved inside the disk (KK00). Assumption that the disk density decreases smoothly to zero towards the disk surface greatly simplifies the solution. We can not use such an assumption in the magnetic case. There, a back reaction from the disk towards the magnetosphere, with the ongoing magnetic reconnection, greatly complicates the solution. This is why in a magnetic case we can obtain only the most general conditions, not the solution.

We search for stationary ($\partial/\partial t = 0$), and axially symmetric ($\partial/\partial \varphi = 0$) solutions[6]. We also assume the symmetry under reflection about the z=0 midplane. Then physical quantities like Ω, ρ, P, η, $u = v_{\mathrm{r}}$, and c are even functions of z, while $v = v_z$ is odd under reflections through the equatorial plane. When we expand an even/odd function (e.g. Ω) in powers of $\epsilon << 1$ we require each term in the expansion (e.g. Ω_i; i = 0, 1,

[6]Sometimes we write $\partial/\partial x = \partial_x$ for simplification.

2,...) to be independently even/odd. This means that e.g. for $\Omega = \Omega_0 + \epsilon\Omega_1 + \epsilon^2\Omega_2 + \epsilon^3\Omega_3 + \dots$, when we have Ω =even, all the terms, including ϵ in $(\epsilon\Omega_n)$, should be even =¿ $\epsilon\Omega_1 = 0 = \Omega_1 = 0$ and so on for all the odd terms. This is generalized in Rebusco et al. (2009) [Reb+09].

We work in the cylindrical coordinates (r, φ, z). The normalization is defined with the following equations: $\epsilon = \tilde{c}_\mathrm{s}/(\tilde{R}\tilde{\Omega}) = \tilde{H}/\tilde{R} \ll 1$, so that $\tilde{c}_\mathrm{s} = \epsilon\tilde{R}\tilde{\Omega}$, and then $c_s' = c_s/\tilde{c}_\mathrm{s} = c_s/(\epsilon\tilde{R}\tilde{\Omega})$. Twiddles denote characteristic values of the variables, and primes the scaled variables. Further, $\Omega' = \Omega/\tilde{\Omega}$, $\tilde{\Omega} = \Omega_\mathrm{K} = \sqrt{GM_\star/\tilde{R}^3}$, $r' = r/\tilde{R}$, $z' = z/(\epsilon\tilde{R})$, $v_r' = v_r/\tilde{c}_\mathrm{s} = v_r/(\epsilon\tilde{R}\tilde{\Omega})$, $v_z' = v_z/\tilde{c}_\mathrm{s} = v_z/(\epsilon\tilde{R}\tilde{\Omega})$, $v_\varphi' = v_\varphi/(\tilde{R}\tilde{\Omega})$. The magnetic field we normalize with the Alfvén speed $\tilde{v}_\mathrm{A} = \tilde{B}/\sqrt{4\pi\tilde{\rho}}$ as a characteristic speed, and $\rho' = \rho/\tilde{\rho}$. Then we have $B' = B/\tilde{B} = B/(\tilde{v}_\mathrm{A}^2\sqrt{4\pi\tilde{\rho}})$, and $\tilde{B}$ is the normalization for all the magnetic field components: $B_r' = B_r/\tilde{B}$, $B_z' = B_z/\tilde{B}$, $B_\varphi' = B_\varphi/\tilde{B}$.

The beta plasma parameter $\beta = P_\mathrm{gas}/P_\mathrm{mag} = 8\pi P_\mathrm{gas}/B^2$. With $P = P_\mathrm{gas}$ we can write $c_s^2 = \gamma P/\rho = \gamma\beta B^2/(8\pi\rho) = \gamma\beta v_\mathrm{A}^2/2$, so that $\tilde{v}_\mathrm{A}^2/\tilde{c}_\mathrm{s}^2 = 2/(\gamma\tilde{\beta})$.

The viscosity scales with the sound speed as a characteristic velocity and the height of the disk H, so that the normalization for the kinetic viscosity is $\tilde{\nu}_\mathrm{v} = \tilde{c}_\mathrm{s}\tilde{H} = \epsilon^2\tilde{R}^2\tilde{\Omega}$, and then $\tilde{\eta} = \tilde{\rho}\tilde{\nu}_\mathrm{v} = \tilde{\rho}\epsilon^2\tilde{R}^2\tilde{\Omega}$. Then $\eta' = \eta/\tilde{\eta} = \eta/(\tilde{\rho}\epsilon^2\tilde{R}^2\tilde{\Omega})$. For the resistivity we choose the normalization with the Alfvén speed as a characteristic speed, so that $\tilde{\eta}_\mathrm{m} = \tilde{v}_\mathrm{A}\tilde{H} = \epsilon\tilde{R}\tilde{v}_\mathrm{A}$. Then $\eta_\mathrm{m}' = \eta_\mathrm{m}/\tilde{\eta}_\mathrm{m} = \eta_\mathrm{m}/(\epsilon\tilde{R}\tilde{v}_\mathrm{A}) = \eta_\mathrm{m}\sqrt{\gamma\tilde{\beta}/2}\,/(\tilde{c}_\mathrm{s}\epsilon\tilde{R}) = \eta_\mathrm{m}\sqrt{\gamma\tilde{\beta}/2}\,/(\epsilon^2\tilde{R}^2\tilde{\Omega})$.

We write the normalized equations of continuity, magnetic field solenoidality ($\nabla\cdot\mathbf{B} = 0$), momentum, induction and energy density. For simplicity, in some cases we use the notation $\partial_x = \partial/\partial x$, and we drop all primes in the following (where all the variables are scaled, so no confusion can arise). In the results, $a = f(r)$, and $b = f(r)$ do *not* imply $a(r,z) \equiv b(r,z)$, we just denote a *generic* radial function as $f(r)$, without implying any particular functional dependence on r.

We illustrate the asymptotic approximation method in detail by deriving all the terms through the second order in the continuity equation. Other equations are derived by following the same method.

Equation of continuity:

The continuity equation is:

$$\frac{\partial\rho}{\partial t} + \nabla\cdot(\rho\mathbf{v}) = 0. \tag{3.7}$$

In the stationary case $\partial_t\rho = 0$. With the condition of axial symmetry $\partial_\varphi(\rho\mathbf{v}) = 0$:

$$\frac{1}{r}\partial_r(r\rho v_r) + \partial_z(\rho v_z) = 0. \tag{3.8}$$

The normalized equation, with the terms in the order of a small parameter ϵ:

$$\frac{1}{\tilde{R}r'}\frac{1}{\tilde{R}}\partial_{r'}(r'\tilde{R}\tilde{\rho}\rho'\epsilon\tilde{\Omega}\tilde{R}v_r') + \frac{1}{\epsilon\tilde{R}}\partial_{z'}(\rho\tilde{\rho}\epsilon\tilde{\Omega}\tilde{R}v_z') = 0. \tag{3.9}$$

Dividing through $\tilde{\rho}\tilde{\Omega}$ and removing the primes, we can write:

$$\frac{\epsilon}{r}\partial_r(r\rho v_r) + \partial_z(\rho v_z) = 0. \tag{3.10}$$

With the expansion in ϵ in each quantity:

$$\begin{aligned}\frac{\epsilon}{r}\partial_r[r(\rho_0 + \epsilon\rho_1 + \epsilon^2\rho_2 + \dots)(v_{r0} + \epsilon v_{r1} + \epsilon^2\rho_2 + \dots)]\\ +\partial_z[(\rho_0 + \epsilon\rho_1 + \epsilon^2\rho_2 + \dots)(v_{z0} + \epsilon v_{z1} + \epsilon^2 v_{z2} + \dots)] = 0.\end{aligned} \tag{3.11}$$

Now we can write the terms in the different orders in ϵ.

Order ϵ^0:

$$\frac{\partial}{\partial z}\left(\rho_0 v_{z0}\right) = 0 \;\Rightarrow v_{z0} \equiv 0. \tag{3.12}$$

Since ρ_0 is an even function, and v_z is odd with respect to z, at the disk equatorial plane this product is $\rho_0 v_{z0} = 0$. Since it does not depend on z, and $\rho_0 \neq 0$, we conclude that $v_{z0} = 0$ throughout the disk.

Order ϵ^1:

In the first order in ϵ it is:

$$\frac{1}{r}\frac{\partial}{\partial r}\left(r\rho_0 v_{r0}\right) + \frac{\partial}{\partial z}\left(\rho_0 v_{z1}\right) = 0 \;\Rightarrow v_{z1} \equiv 0. \tag{3.13}$$

Since $v_{r0} \equiv 0$ (KK00), we have $\partial_z(\rho_0 v_{z1}) = 0 \Rightarrow \rho_0 v_{z1} = \text{const}$ along z. Since v_z is odd with respect to z, following the same argumentation as above in the zeroth order term in ϵ, we conclude that $v_{z1} = 0$ everywhere.

Order ϵ^2:

In the second order in ϵ:

$$\frac{1}{r}\frac{\partial}{\partial r}\left(r\rho_0 v_{r1}\right) + \frac{\partial}{\partial z}\left(\rho_0 v_{z2}\right) = 0. \tag{3.14}$$

Finding the solution for v_{r1} will give us the vertical dependence of v_{z2}.

The same procedure is carried in each of the following equations.

Magnetic field solenoidality ($\nabla \cdot \mathbf{B} = 0$):

$$\frac{\epsilon}{r}\frac{\partial}{\partial r}\left(rB_r\right) + \frac{\partial B_z}{\partial z} = 0 \tag{3.15}$$

Order ϵ^0:

$$\frac{\partial B_{z0}}{\partial z} = 0 \;\Rightarrow B_{z0} = f(r) \text{ or } B_{z0} = 0. \tag{3.16}$$

Order ϵ^1:

$$\frac{1}{r}\frac{\partial}{\partial r}\left(rB_{r0}\right) + \frac{\partial B_{z1}}{\partial z} = 0. \tag{3.17}$$

Order ϵ^2:

$$\frac{1}{r}\frac{\partial}{\partial r}\left(rB_{r1}\right) + \frac{\partial B_{z2}}{\partial z} = 0 \tag{3.18}$$

Radial momentum:

$$\begin{aligned}\epsilon^2 v_r\frac{\partial v_r}{\partial r}+\epsilon v_z\frac{\partial v_r}{\partial z}-\Omega^2 r=&-\frac{1}{r^2}\left[1+\epsilon^2\left(\frac{z}{r}\right)^2\right]^{-3/2}\\ -\epsilon^2 n\frac{\partial c_{\rm s}^2}{\partial r}+&\frac{2}{\gamma\tilde{\beta}}\frac{1}{\rho}\left(\epsilon^2 B_r\frac{\partial B_r}{\partial r}+\epsilon B_z\frac{\partial B_r}{\partial z}-\epsilon^2\frac{B_\varphi^2}{r}\right)\\ -\frac{\epsilon^2}{\gamma\tilde{\beta}}\frac{1}{\rho}\frac{\partial B^2}{\partial r}+&\frac{\epsilon^3}{\rho r}\frac{\partial}{\partial r}\left(2\eta r\frac{\partial v_r}{\partial r}\right)+\frac{\epsilon}{\rho}\frac{\partial}{\partial z}\left(\eta\frac{\partial v_r}{\partial z}\right)\\ +\frac{\epsilon^2}{\rho}\frac{\partial}{\partial z}\left(\eta\frac{\partial v_z}{\partial r}\right)-\epsilon^3\frac{2\eta v_r}{\rho r^2}-&\frac{2\epsilon^3}{3\rho}\frac{\partial}{\partial r}\left[\eta\frac{1}{r}\frac{\partial}{\partial r}\left(rv_r\right)\right]\\ &-\frac{2}{3}\frac{\epsilon^2}{\rho}\frac{\partial}{\partial r}\left(\eta\frac{\partial v_z}{\partial z}\right).\end{aligned}\tag{3.19}$$

For an ideal gas with the polytropic index n, if adiabatic index $\gamma = 5/3$, we have $n = 3/2$.

Order ϵ^0:

$$\Omega_0 = r^{-3/2}\tag{3.20}$$

Order ϵ^1:

$$-2r\Omega_0\Omega_1=\frac{2}{\gamma\tilde{\beta}}\frac{1}{\rho_0}B_{z0}\frac{\partial B_{r0}}{\partial z}+\frac{1}{\rho_0}\frac{\partial}{\partial z}\left(\eta_0\frac{\partial v_{r0}}{\partial z}\right)\tag{3.21}$$

Since $v_{r0}\equiv 0$, from the vertical symmetry $\Omega_1 = 0$ follows, as shown in KK00 for the HD disk, see also Appendix A in Rebusco (2009) [Reb+09] for a more formal derivation[7].

Order ϵ^2:

$$\begin{aligned}2r\rho_0\Omega_0\Omega_2=&\frac{3\rho_0}{2}\frac{z^2}{r^4}+n\rho_0\frac{\partial c_{s0}^2}{\partial r}-\frac{\partial}{\partial z}\left(\eta_0\frac{\partial v_{r1}}{\partial z}\right)\\ -\frac{2}{\gamma\tilde{\beta}}&\left(B_{r0}\frac{\partial B_{r0}}{\partial r}+B_{z0}\frac{\partial B_{r1}}{\partial z}+B_{z1}\frac{\partial B_{r0}}{\partial z}-\frac{B_{\varphi 0}^2}{r}\right)\\ &+\frac{1}{\gamma\tilde{\beta}}\frac{\partial B_0^2}{\partial r}.\end{aligned}\tag{3.23}$$

Azimuthal momentum:

$$\begin{aligned}\epsilon\frac{\rho v_r}{r^2}\frac{\partial}{\partial r}\left(r^2\Omega\right)+\rho v_z\frac{\partial\Omega}{\partial z}=&\frac{\epsilon^2}{r^3}\frac{\partial}{\partial r}\left(r^3\eta\frac{\partial\Omega}{\partial r}\right)+\frac{\partial}{\partial z}\left(\eta\frac{\partial\Omega}{\partial z}\right)\\ &+\frac{2}{\gamma\tilde{\beta}}\frac{1}{r}\left(\epsilon^2 B_r\frac{\partial B_\varphi}{\partial r}+\epsilon B_z\frac{\partial B_\varphi}{\partial z}+\epsilon^2\frac{B_\varphi B_r}{r}\right)\end{aligned}\tag{3.24}$$

[7] If this is maintained in the MHD case, we can write, with $v_{r0}=0$:

$$B_{z0}\frac{\partial B_{r0}}{\partial z}=0.\tag{3.22}$$

.

Order ϵ^0:

$$0 = \frac{\partial}{\partial z}\left(\eta_0 \frac{\partial \Omega_0}{\partial z}\right), \tag{3.25}$$

consistent with Eq. (3.20).

Order ϵ^1:

$$\frac{\rho_0 v_{r0}}{r^2}\frac{\partial}{\partial r}\left(r^2\Omega_0\right) = \frac{\partial}{\partial z}\left(\eta_0 \frac{\partial \Omega_1}{\partial z}\right) + \frac{2}{\gamma\tilde{\beta}}\frac{1}{r}B_{z0}\frac{\partial B_{\varphi 0}}{\partial z} \tag{3.26}$$

Since $v_{r0} = \Omega_1 = 0$, we obtain that:

$$B_{z0}\frac{\partial B_{\varphi 0}}{\partial z} = 0. \tag{3.27}$$

Order ϵ^2:

$$\begin{aligned}\frac{\rho_0 v_{r1}}{r}\frac{\partial}{\partial r}\left(r^2\Omega_0\right) = \frac{2}{\gamma\tilde{\beta}}\left(B_{r0}\frac{\partial B_{\varphi 0}}{\partial r} + B_{z0}\frac{\partial B_{\varphi 1}}{\partial z} + \frac{B_{r0}B_{\varphi 0}}{r}\right) \\ + \frac{1}{r^2}\frac{\partial}{\partial r}\left(r^3\eta_0\frac{\partial \Omega_0}{\partial r}\right) + \frac{\partial}{\partial z}\left(\eta_0\frac{\partial \Omega_2}{\partial z}\right).\end{aligned} \tag{3.28}$$

Vertical momentum:

$$\begin{aligned}\epsilon v_r\frac{\partial v_z}{\partial r} + v_z\frac{\partial v_z}{\partial z} = -\frac{z}{r^3}\left[1+\epsilon^2\left(\frac{z}{r}\right)^2\right]^{-3/2} \\ -n\frac{\partial c_s^2}{\partial z} + \frac{2}{\gamma\tilde{\beta}}\frac{1}{\rho}\left(\epsilon B_r\frac{\partial B_z}{\partial r} + B_z\frac{\partial B_z}{\partial z}\right) - \frac{1}{\gamma\tilde{\beta}}\frac{1}{\rho}\frac{\partial B^2}{\partial z} \\ + \frac{2}{\rho}\frac{\partial}{\partial z}\left(\eta\frac{\partial v_z}{\partial z}\right) + \frac{\epsilon^2}{\rho r}\frac{\partial}{\partial r}\left(r\eta\frac{\partial v_z}{\partial r}\right) \\ -\frac{2}{3}\frac{\epsilon}{\rho}\frac{\partial}{\partial z}\left[\frac{\eta}{r}\frac{\partial}{\partial r}\left(rv_r\right)\right] - \frac{2}{3\rho}\frac{\partial}{\partial z}\left(\eta\frac{\partial v_z}{\partial z}\right) \\ + \frac{\epsilon}{\rho r}\frac{\partial}{\partial r}\left(\eta r\frac{\partial v_r}{\partial z}\right)\end{aligned} \tag{3.29}$$

Order ϵ^0:

$$0 = -\frac{z}{r^3} - n\frac{\partial c_{s0}^2}{\partial z} - \frac{1}{\gamma\tilde{\beta}}\frac{1}{\rho_0}\frac{\partial B_0^2}{\partial z}. \tag{3.30}$$

From Eqs. (3.16), (3.22) and (3.27), with $B_{z0} = f(r)$ it follows that $B_{r0} = f(r)$ and $B_{\varphi 0} = f(r)$. With $B_0^2 = B_{r0}^2 + B_{z0}^2 + B_{\varphi 0}^2$ it gives $\partial_z B_0^2 = 0 = \partial_z B_0$. For a disk in the vertical equilibrium, components of the magnetic field do not contribute in the zeroth order in ϵ to the vertical gradient of the magnetic field.

We remain with the vertical hydrostatic equilibrium equation identical to the purely HD case:

$$\frac{z}{r^3} = -n\frac{\partial c_{s0}^2}{\partial z}. \tag{3.31}$$

This is consistent with the demand that, for a quasi-stationary disk, the lowest order in ϵ of the magnetic field components does not contribute to the solution:

$$B_{r0} = B_{z0} = B_{\varphi 0} = 0 \;\; \Rightarrow B_0 = 0. \tag{3.32}$$

Order ϵ^1:

$$\begin{aligned} \frac{2}{\gamma\tilde{\beta}}\left[B_{z0}\frac{\partial B_{z1}}{\partial z} - \frac{\partial}{\partial z}\left(B_0 B_1\right)\right] - \frac{2}{3r}\frac{\partial}{\partial z}\left[\eta_0 \frac{\partial}{\partial r}\left(r v_{r1}\right)\right] \\ + \frac{1}{r}\frac{\partial}{\partial r}\left(\eta_0 r \frac{\partial v_{r1}}{\partial z}\right) = 0. \end{aligned} \tag{3.33}$$

With $B_{z0} = B_0 = 0$ we obtain:

$$\frac{\partial}{\partial z}\left[\eta_0 \frac{\partial}{\partial r}\left(r v_{r1}\right)\right] = \frac{3}{2}\frac{\partial}{\partial r}\left(\eta_0 r \frac{\partial v_{r1}}{\partial z}\right). \tag{3.34}$$

Order ϵ^2:

$$\begin{aligned} 0 = B_{r0}\frac{\partial B_{z1}}{\partial r} + B_{r1}\frac{\partial B_{z0}}{\partial r} + B_{z0}\frac{\partial B_{z2}}{\partial z} + B_{z1}\frac{\partial B_{z1}}{\partial z} \\ + \frac{1}{\gamma\tilde{\beta}}\frac{\partial}{\partial z}\left(B_1^2 + 2B_0 B_2\right) + \frac{2}{3}\frac{\partial}{\partial z}\left[\frac{\eta_1}{r}\frac{\partial}{\partial r}\left(r v_{r1}\right)\right] \\ -2\frac{\partial}{\partial z}\left(\eta_0 v_{z2}\right) + \frac{2}{3}\frac{\partial}{\partial z}\left(\eta_0 \frac{\partial v_{z2}}{\partial z}\right) - \frac{1}{r}\frac{\partial}{\partial r}\left(\eta_0 r \frac{\partial v_{r1}}{\partial z}\right). \end{aligned} \tag{3.35}$$

If now we use Eq. (3.17) with $B_{r0} = 0$, giving

$$\frac{\partial B_{z1}}{\partial z} = 0, \tag{3.36}$$

we obtain:

$$\begin{aligned} \frac{3\rho_0}{2}\frac{z^3}{r^7} = 2n\rho_0\frac{\partial}{\partial z}\left(c_{s0}c_{s2}\right) + n\rho_2\frac{\partial c_{s0}^2}{\partial z} + \frac{1}{\gamma\tilde{\beta}}\frac{\partial B_1^2}{\partial z} \\ -2\frac{\partial}{\partial z}\left(\eta_0 v_{z2}\right) + \frac{2}{3}\frac{\partial}{\partial z}\left[\frac{\eta_1}{r}\frac{\partial}{\partial r}\left(r v_{r1}\right)\right] + \frac{2}{3}\frac{\partial}{\partial z}\left(\eta_0\frac{\partial v_{z2}}{\partial z}\right) \\ -\frac{1}{r}\frac{\partial}{\partial r}\left(\eta_0 r\frac{\partial v_{r1}}{\partial z}\right). \end{aligned} \tag{3.37}$$

3.2.1 B0=0 solutions

We review already obtained results with the vanishing com- ponents of B0 , when magnetic field influences the solution only in the higher orders in ϵ. Then Eqs. (3.14), (3.23) and (3.28) become the same as in a HD case:

$$\begin{aligned} \frac{1}{r}\frac{\partial}{\partial r}\left(r\rho_0 v_{r1}\right) + \frac{\partial}{\partial z}\left(\rho_0 v_{z2}\right) = 0. \\ 2r\rho_0\Omega_0\Omega_2 = \frac{3\rho_0}{2}\frac{z^2}{r^4} + n\rho_0\frac{\partial c_{s0}^2}{\partial r} - \frac{\partial}{\partial z}\left(\eta_0\frac{\partial v_{r1}}{\partial z}\right) \\ \frac{\rho_0 v_{r1}}{r}\frac{\partial}{\partial r}\left(r^2\Omega_0\right) = \frac{1}{r^2}\frac{\partial}{\partial r}\left(r^3\eta_0\frac{\partial\Omega_0}{\partial r}\right) + \frac{\partial}{\partial z}\left(\eta_0\frac{\partial\Omega_2}{\partial z}\right). \end{aligned} \tag{3.38}$$

In the disk solution in [Hōs77] and KK00, those equations were solved by assuming that the disk density decreases towards the surface, $\rho_0 \to 0$. If, instead, we supply at the disk surface a value at the boundary with the coronal density $\rho_{\rm cd}$, we obtain:

$$\rho_0 = \left(\rho_{\rm cd}^{2/3} + \frac{h^2 - z^2}{5r^3}\right)^{3/2}, \tag{3.39}$$

where h is the disk semi-thickness. The pressure and sound speed now become:

$$P_0 = \left(\rho_{\rm cd}^{2/3} + \frac{h^2 - z^2}{5r^3}\right)^{5/2}, c_{\rm s0} = \sqrt{\frac{5}{3}\left(\rho_{\rm cd}^{2/3} + \frac{h^2 - z^2}{5r^3}\right)}. \tag{3.40}$$

The [Hōs77] solution is recovered by setting $\rho_{\rm cd} = 0$, for the boundary at the disk maximal height.

In our case, since $h \propto r$, we can write, with the proportionality constant h', $h = h'r$. Assuming the corona at the surface of the disk to be in the hydrostatic equilibrium, with $\rho_{cd} \propto (\rho_{\rm c0}/r)^{3/2}$ we can write:

$$\begin{aligned} c_{\rm s0}^2 &= \frac{5}{3}\left(\rho_{cd}^{2/3} + \frac{h'^2 r^2 - z^2}{5r^3}\right) = \frac{5}{3}\left(\frac{k_\rho \rho_{\rm c0}}{r} + \frac{h'^2}{5r} - \frac{z^2}{5r^3}\right) \\ &= \frac{5k_\rho\rho_{\rm c0} + h'^2}{3r}\left[1 - \left(\zeta\frac{z}{r}\right)^2\right] \propto \frac{1}{r}\left[1 - \left(\zeta\frac{z}{r}\right)^2\right], \end{aligned} \tag{3.41}$$

with $\zeta^2 = 1/(5k_\rho\rho_{\rm c0} + h'^2)$, where k_ρ is the proportionality constant, and $\rho_{\rm c0} \sim 0.01$ is the ratio between the initial corona and disk density.

Now we can continue with the rest of equations.

Radial induction equation:

$$\begin{aligned} 0 = {} & B_z\frac{\partial v_r}{\partial z} + v_r\frac{\partial B_z}{\partial z} - B_r\frac{\partial v_z}{\partial z} - v_z\frac{\partial B_r}{\partial z} \\ & + \sqrt{\frac{2}{\gamma\tilde{\beta}}}\left(\frac{\partial \eta_{\rm m}}{\partial z}\frac{\partial B_r}{\partial z} - \epsilon\frac{\partial \eta_{\rm m}}{\partial z}\frac{\partial B_z}{\partial r}\right) \\ & + \eta_{\rm m}\sqrt{\frac{2}{\gamma\tilde{\beta}}}\left(\frac{\partial^2 B_r}{\partial z^2} - \epsilon\frac{\partial^2 B_z}{\partial r \partial z}\right). \end{aligned} \tag{3.42}$$

Order ϵ^0:

$$\frac{\partial \eta_{\rm m0}}{\partial z}\frac{\partial B_{r0}}{\partial z} + \eta_{\rm m0}\frac{\partial^2 B_{r0}}{\partial z^2} = 0. \tag{3.43}$$

If we multiply this with B_{z0}, the first term equals zero because of Eq. (3.22), and we remain with the second term:

$$\eta_{\rm m0} B_{z0}\frac{\partial^2 B_{r0}}{\partial z^2} = 0. \tag{3.44}$$

If all the zeroth-order magnetic field components are zero, $B_{r0} = 0$ and we remain with $0 = 0$

Order ϵ^1:

$$\begin{aligned} B_{z0}\frac{\partial v_{r1}}{\partial z} + \sqrt{\frac{2}{\gamma\tilde{\beta}}}\Bigg(\frac{\partial \eta_{\mathrm{m}0}}{\partial z}\frac{\partial B_{r1}}{\partial z} + \frac{\partial \eta_{\mathrm{m}1}}{\partial z}\frac{\partial B_{r0}}{\partial z} \\ -\frac{\partial \eta_{\mathrm{m}0}}{\partial z}\frac{\partial B_{z0}}{\partial r}\Bigg) + \sqrt{\frac{2}{\gamma\tilde{\beta}}}\Bigg(\eta_{\mathrm{m}0}\frac{\partial^2 B_{r1}}{\partial z^2} + \eta_{\mathrm{m}1}\frac{\partial^2 B_{r0}}{\partial z^2} \\ -\eta_{\mathrm{m}0}\frac{\partial^2 B_{z0}}{\partial r \partial z}\Bigg) = 0. \end{aligned} \tag{3.45}$$

With the components of B_0 vanishing, we remain with:

$$\frac{\partial}{\partial z}\left(\eta_{\mathrm{m}0}\frac{\partial B_{r1}}{\partial z}\right) = 0. \tag{3.46}$$

Order ϵ^2:

$$\begin{aligned} 0 = B_{z0}\frac{\partial v_{r2}}{\partial z} + B_{z1}\frac{\partial v_{r1}}{\partial z} + v_{r1}\frac{\partial B_{z1}}{\partial z} - B_{r0}\frac{\partial v_{z2}}{\partial z} \\ -v_{z2}\frac{\partial B_{r0}}{\partial z} + \sqrt{\frac{2}{\gamma\tilde{\beta}}}\Bigg(\frac{\partial \eta_{\mathrm{m}0}}{\partial z}\frac{\partial B_{r2}}{\partial z} + \frac{\partial \eta_{\mathrm{m}1}}{\partial z}\frac{\partial B_{r1}}{\partial z} \\ +\frac{\partial \eta_{\mathrm{m}2}}{\partial z}\frac{\partial B_{r0}}{\partial z} - \frac{\partial \eta_{\mathrm{m}1}}{\partial r}\frac{\partial B_{z0}}{\partial r} - \frac{\partial \eta_{\mathrm{m}0}}{\partial z}\frac{\partial B_{z1}}{\partial r}\Bigg) \\ +\sqrt{\frac{2}{\gamma\tilde{\beta}}}\Bigg(\eta_{\mathrm{m}0}\frac{\partial^2 B_{r2}}{\partial z^2} + \eta_{\mathrm{m}1}\frac{\partial^2 B_{r1}}{\partial z^2} - \eta_{\mathrm{m}0}\frac{\partial^2 B_{z1}}{\partial r \partial z} \\ -\eta_{\mathrm{m}1}\frac{\partial^2 B_{z0}}{\partial r \partial z}\Bigg). \end{aligned} \tag{3.47}$$

Without the components of B_0, we remain with:

$$\begin{aligned} 0 = B_{z1}\frac{\partial v_{r1}}{\partial z} + \sqrt{\frac{2}{\gamma\tilde{\beta}}}\Bigg(\frac{\partial \eta_{\mathrm{m}0}}{\partial z}\frac{\partial B_{r2}}{\partial z} + \frac{\partial \eta_{\mathrm{m}1}}{\partial z}\frac{\partial B_{r1}}{\partial z} \\ -\frac{\partial \eta_{\mathrm{m}0}}{\partial z}\frac{\partial B_{z1}}{\partial r} + \eta_{\mathrm{m}0}\frac{\partial^2 B_{r2}}{\partial z^2} + \eta_{\mathrm{m}1}\frac{\partial^2 B_{r1}}{\partial r^2} - \eta_{\mathrm{m}0}\frac{\partial B_{z2}}{\partial r \partial z}\Bigg). \end{aligned} \tag{3.48}$$

Azimuthal induction equation:

$$\begin{aligned} 0 = \epsilon r B_r\frac{\partial \Omega}{\partial r} + \epsilon r\Omega\frac{\partial B_r}{\partial r} + \epsilon\Omega B_r + r B_z\frac{\partial \Omega}{\partial z} + r\Omega\frac{\partial B_z}{\partial z} \\ -\epsilon^2 v_r\frac{\partial B_\varphi}{\partial r} - \epsilon v_z\frac{\partial B_\varphi}{\partial z} - \epsilon^2 B_\varphi\frac{\partial v_r}{\partial r} - \epsilon B_\varphi\frac{\partial v_z}{\partial z} \\ +\sqrt{\frac{2}{\gamma\tilde{\beta}}}\left(\frac{\epsilon^3 B_\varphi}{r}\frac{\partial \eta_{\mathrm{m}}}{\partial r} + \epsilon^3\frac{\partial \eta_{\mathrm{m}}}{\partial r}\frac{\partial B_\varphi}{\partial r} + \epsilon\frac{\partial \eta_{\mathrm{m}}}{\partial z}\frac{\partial B_\varphi}{\partial z}\right) \\ +\eta_{\mathrm{m}}\sqrt{\frac{2}{\gamma\tilde{\beta}}}\left(\frac{\epsilon^3}{r}\frac{\partial B_\varphi}{\partial r} - \frac{\epsilon^3 B_\varphi}{r^2} + \epsilon^3\frac{\partial^2 B_\varphi}{\partial r^2} + \epsilon\frac{\partial^2 B_\varphi}{\partial z^2}\right). \end{aligned} \tag{3.49}$$

Order ϵ^0:

$$r\Omega_0\frac{\partial B_{z0}}{\partial z}=0\Rightarrow\frac{\partial B_{z0}}{\partial z}=0, \tag{3.50}$$

in agreement with Eq. (3.16).

Order ϵ^1:

$$\begin{aligned} &rB_{r0}\frac{\partial\Omega_0}{\partial r}+r\Omega_0\frac{\partial B_{r0}}{\partial r}+r\Omega_0\frac{\partial B_{z1}}{\partial z}\\ &+\sqrt{\frac{2}{\gamma\tilde{\beta}}}\left(\frac{\partial\eta_{\mathrm{m}0}}{\partial z}\frac{\partial B_{\varphi0}}{\partial z}+\eta_{\mathrm{m}0}\frac{\partial^2B_{\varphi0}}{\partial z^2}\right)=0, \end{aligned} \tag{3.51}$$

which, with vanishing components of B_0, becomes:

$$r\Omega_0\frac{\partial B_{z1}}{\partial z}=0. \tag{3.52}$$

This confirms Eq. (3.36).

Order ϵ^2:

$$\begin{aligned} 0=&r\frac{\partial B_{r1}}{\partial r}\frac{\partial\Omega_0}{\partial r}+r\Omega_0\frac{\partial B_{r1}}{\partial r}+rB_{z0}\frac{\partial\Omega_2}{\partial z}+r\Omega_0\frac{\partial B_{z2}}{\partial z}\\ &+\sqrt{\frac{2}{\gamma\tilde{\beta}}}\left(\frac{\partial\eta_{\mathrm{m}1}}{\partial z}\frac{\partial B_{\varphi0}}{\partial z}+\frac{\partial\eta_{\mathrm{m}0}}{\partial z}\frac{\partial B_{\varphi1}}{\partial z}+\eta_{\mathrm{m}0}\frac{\partial^2B_{\varphi1}}{\partial z^2}\right.\\ &\left.+\eta_{\mathrm{m}1}\frac{\partial^2B_{\varphi0}}{\partial z^2}\right). \end{aligned} \tag{3.53}$$

Without the vanishing components of B_0 it becomes:

$$\begin{aligned} &r\frac{\partial B_{r1}}{\partial r}\frac{\partial\Omega_0}{\partial r}+r\Omega_0\frac{\partial B_{r1}}{\partial r}+r\Omega_0\frac{\partial B_{z2}}{\partial z}\\ &+\sqrt{\frac{2}{\gamma\tilde{\beta}}}\left(\frac{\partial\eta_{\mathrm{m}0}}{\partial z}\frac{\partial B_{\varphi1}}{\partial z}+\eta_{\mathrm{m}0}\frac{\partial^2B_{\varphi1}}{\partial z^2}\right)=0. \end{aligned} \tag{3.54}$$

Vertical induction equation:

$$\begin{aligned} 0=&\frac{v_zB_r}{r}-\frac{v_rB_z}{r}+B_r\frac{\partial v_z}{\partial r}-v_r\frac{\partial B_z}{\partial r}+v_z\frac{\partial B_r}{\partial r}\\ &-B_z\frac{\partial v_r}{\partial r}+\sqrt{\frac{2}{\gamma\tilde{\beta}}}\left(\epsilon\frac{\partial\eta_{\mathrm{m}}}{\partial r}\frac{\partial B_z}{\partial r}-\frac{\partial\eta_{\mathrm{m}}}{\partial r}\frac{\partial B_r}{\partial z}\right)\\ &+\eta_{\mathrm{m}}\sqrt{\frac{2}{\gamma\tilde{\beta}}}\left(\frac{\epsilon}{r}\frac{\partial B_z}{\partial r}-\frac{1}{r}\frac{\partial B_r}{\partial r}-\frac{\partial^2B_r}{\partial r\partial z}+\epsilon\frac{\partial^2B_z}{\partial r^2}\right). \end{aligned} \tag{3.55}$$

Order ϵ^0:

$$\eta_{\mathrm{m}0}\left(\frac{1}{r}\frac{\partial B_{r0}}{\partial r}+\frac{\partial^2B_{r0}}{\partial r\partial z}\right)+\frac{\partial\eta_{\mathrm{m}0}}{\partial r}\frac{\partial B_{r0}}{\partial z}=0, \tag{3.56}$$

giving, with $B_{r0}=0$ that $0=0$

Order ϵ^1:

$$\begin{aligned} & v_{r1}\left(\frac{B_{z0}}{r}+\frac{\partial B_{z0}}{\partial r}\right)+B_{z0}\frac{v_{r1}}{\partial r} \\ =\sqrt{\frac{2}{\gamma\tilde{\beta}}}\Bigg[& \frac{\partial\eta_{\mathrm{m}0}}{\partial r}\left(\frac{\partial B_{z0}}{\partial r}-\frac{\partial B_{r1}}{\partial z}\right)-\frac{\partial\eta_{\mathrm{m}1}}{\partial r}\frac{\partial B_{r0}}{\partial z} \\ & +\frac{\eta_{\mathrm{m}0}}{r}\left(\frac{\partial B_{z0}}{\partial r}-\frac{\partial B_{r1}}{\partial r}\right)-\eta_{\mathrm{m}0}\frac{\partial^2 B_{r1}}{\partial r\partial z} \\ & -\eta_{\mathrm{m}1}\left(\frac{1}{r}\frac{\partial B_{r0}}{\partial r}+\frac{\partial^2 B_{r0}}{\partial r\partial z}\right)\Bigg]. \end{aligned} \tag{3.57}$$

With vanishing components of B_0:

$$\frac{\partial}{\partial r}\left(\eta_{\mathrm{m}0}\frac{\partial B_{r1}}{\partial z}\right)+\frac{\eta_{\mathrm{m}0}}{r}\frac{\partial B_{r1}}{\partial r}=0. \tag{3.58}$$

Order ϵ^2:

$$\begin{aligned} & \frac{1}{r}\left(v_{z2}B_{r0}-v_{r1}B_{z1}-v_{r2}B_{z0}\right)+B_{r0}\frac{\partial v_{z2}}{\partial r}+v_{z2}\frac{\partial B_{r0}}{\partial r} \\ & -\left(B_{z0}\frac{\partial v_{r2}}{\partial r}+v_{r2}\frac{\partial B_{z0}}{\partial r}\right)-\left(B_{z1}\frac{\partial v_{r1}}{\partial r}+v_{r1}\frac{\partial B_{z1}}{\partial r}\right) \\ & =\sqrt{\frac{2}{\gamma\tilde{\beta}}}\Bigg[\frac{\partial\eta_{\mathrm{m}0}}{\partial r}\left(\frac{\partial B_{r2}}{\partial z}-\frac{\partial B_{z1}}{\partial r}\right)+\frac{\partial\eta_{\mathrm{m}1}}{\partial r}\left(\frac{\partial B_{r1}}{\partial z}\right. \\ & \left.-\frac{\partial B_{z0}}{\partial r}\right)+\frac{\partial\eta_{\mathrm{m}2}}{\partial r}\frac{\partial B_{r0}}{\partial z}+\frac{\eta_{\mathrm{m}0}}{r}\left(\frac{\partial B_{r2}}{\partial r}-\frac{\partial B_{z1}}{\partial r}\right) \\ & +\frac{\eta_{\mathrm{m}1}}{r}\left(\frac{\partial B_{r1}}{\partial r}-\frac{\partial B_{z0}}{\partial r}\right)+\frac{\eta_{\mathrm{m}2}}{r}\frac{\partial B_{r0}}{\partial r}+\eta_{\mathrm{m}0}\frac{\partial^2 B_{r2}}{\partial r\partial z} \\ & +\eta_{\mathrm{m}1}\frac{\partial^2 B_{r1}}{\partial r\partial z}+\eta_{\mathrm{m}2}\frac{\partial^2 B_{r0}}{\partial r\partial z}-\eta_{\mathrm{m}0}\frac{\partial^2 B_{z1}}{\partial r^2}-\eta_{\mathrm{m}1}\frac{\partial^2 B_{z0}}{\partial r^2}\Bigg], \end{aligned} \tag{3.59}$$

which with vanishing components of B_0 becomes:

$$\begin{aligned} 0=-\frac{1}{r}v_{r1}B_{z1}-B_{zr1}\frac{\partial v_{r1}}{\partial r}-v_{r2}\frac{\partial B_{z2}}{\partial r} \\ =\sqrt{\frac{2}{\gamma\tilde{\beta}}}\Bigg[& \frac{\partial\eta_{\mathrm{m}0}}{\partial r}\left(\frac{\partial B_{r2}}{\partial z}-\frac{\partial B_{z1}}{\partial r}\right) \\ & +\frac{\eta_{\mathrm{m}0}}{r}\left(\frac{\partial B_{r2}}{\partial r}-\frac{\partial B_{z1}}{\partial r}\right)+\frac{\partial\eta_{\mathrm{m}1}}{\partial r}\frac{\partial B_{r1}}{\partial z} \\ & +\frac{\eta_{\mathrm{m}1}}{r}\frac{\partial B_{r1}}{\partial r}+\eta_{\mathrm{m}0}\frac{\partial^2 B_{r2}}{\partial r\partial z}+\eta_{\mathrm{m}1}\frac{\partial^2 B_{r1}}{\partial r\partial z}-\eta_{\mathrm{m}0}\frac{\partial^2 B_{z1}}{\partial r^2}\Bigg]. \end{aligned} \tag{3.60}$$

Energy equation:

$$\begin{aligned}
&\epsilon^4\tilde{R}^2\tilde{\Omega}^2 n\rho v_r\frac{\partial c_s^2}{\partial r}+\epsilon^3\tilde{R}^2\tilde{\Omega}^2 n\rho v_z\frac{\partial c_s^2}{\partial z}+\epsilon\rho\tilde{v}^2 v_z\frac{\partial v^2/2}{\partial z}\\
&+\epsilon^2\rho\tilde{v}_{\rm A}^2 v_r\frac{\partial v_{\rm A}}{\partial r}+\epsilon\rho\tilde{v}_{\rm A}^2 v_z\frac{\partial v_{\rm A}^2}{\partial z}+\epsilon^2\rho\tilde{v}^2 v_r\frac{\partial v/2}{\partial r}\\
&+\left[\epsilon^2\rho\tilde{\Omega}^2\tilde{R}^2\frac{v_r}{r^2}+\epsilon^3\rho\tilde{\Omega}^2\tilde{R}^2\frac{v_z z}{r^3}\right]\left[1+\epsilon^2\left(\frac{z}{r}\right)^2\right]^{-3/2}\\
&=\frac{\tilde{v}_{\rm A}^2 B_r}{r}\left(\epsilon^2 v_r B_r+\epsilon\Omega r B_\varphi\right)\\
&+\tilde{v}_{\rm A}^2\frac{\partial}{\partial r}\left(\epsilon^2 v_r B_r^2+\epsilon^2 v_z B_z B_r+\epsilon\Omega r B_\varphi B_r\right)\\
&+\tilde{v}_{\rm A}^2\frac{\partial}{\partial z}\left(\epsilon v_r B_r B_z+\epsilon v_z B_z^2+\Omega r B_\varphi B_z\right).
\end{aligned}\tag{3.61}$$

Order ϵ^0:

$$0=\tilde{v}_{\rm A}^2\frac{\partial}{\partial z}(\Omega_0 r B_{\varphi 0}B_{z0})\Rightarrow B_{\varphi 0}\frac{\partial B_{z0}}{\partial z}+B_{z0}\frac{\partial B_{\varphi 0}}{\partial z}=0,$$

which, with the first term vanishing by Eq. (3.16), confirms the Eq. (3.27).

Order ϵ^1:

$$\begin{aligned}
&B_{\varphi 0}\left(\frac{B_{r0}}{2r}+\frac{\partial B_{r0}}{\partial r}+\frac{\partial B_{z1}}{\partial z}\right)+B_{z0}\frac{\partial B_{\varphi 1}}{\partial z}\\
&+B_{r0}\frac{\partial B_{\varphi 0}}{\partial r}+B_{z1}\frac{\partial B_{\varphi 0}}{\partial z}=0.
\end{aligned}\tag{3.62}$$

With Eq. 3.17, we can write:

$$B_{r0}\left(\frac{\partial B_{\varphi 0}}{\partial r}-\frac{B_{\varphi 0}}{2r}\right)+B_{z0}\frac{\partial B_{\varphi 1}}{\partial z}+B_{z1}\frac{\partial B_{\varphi 0}}{\partial z}=0.\tag{3.63}$$

Order ϵ^2:

$$\begin{aligned}
&\Omega_0 B_{r0}B_{\varphi 1}+\frac{\partial}{\partial r}\left[r\Omega_0\left(B_{r0}B_{\varphi 1}+B_{r1}B_{\varphi 0}\right)\right]\\
&+\frac{\partial}{\partial z}\Big[v_{r1}B_{r0}B_{z0}+r\Omega_0\Big(B_{z2}B_{\varphi 0}+B_{z1}B_{\varphi 1}\\
&+B_{z0}B_{\varphi 2}\Big)+r\Omega_2 B_{z0}B_{\varphi 0}\Big]=0,
\end{aligned}\tag{3.64}$$

which with $\partial_z B_{z0}=0$ can be recast into:

$$\begin{aligned}
&\Omega_0 B_{r0}B_{\varphi 1}+\frac{\partial}{\partial r}\left[r\Omega_0\left(B_{r0}B_{\varphi 1}+B_{r1}B_{\varphi 0}\right)\right]\\
&+B_{z0}\frac{\partial}{\partial z}\Big[v_{r1}B_{r0}+r\Big(\Omega_0 B_{\varphi 2}+\Omega_2 B_{\varphi 0}\Big)\Big]=0,
\end{aligned}\tag{3.65}$$

In all three orders in ϵ, with $B_{i0}=0$ with $i=(r,\varphi,z)$ we obtain identities 0=0, confirming that our assumptions and results are in agreement with the energy equation.

We now list the obtained conditions on the solution. In the magnetic case we can only obtain a general set of conditions that should be satisfied in a self-consistent solution.

Expanding the stationary and axi-symmetric normalized analytical equations in the small parameter $\epsilon = H/R$, with the assumed vertical symmetry accross the disk equatorial plane, we find:

• $v_{r0} = v_{z0} = v_{z1} = \Omega_1 = c_{s1} = \rho_1 = 0$, as found in HD case.

• From the radial component of the momentum equation we readily obtain $\Omega_0 = r^{-3/2}$. This solution is valid equally in the HD and MHD cases.

• $B_0 = 0$ and also $B_{i0} = 0$, with $i = (r, \varphi, z)$. Magnetic field influences the disk only in the higher orders in a small parameter ϵ.

• $\partial_z B_{z1} = 0$, vertical dependence of the leading component of the magnetic field in the vertical direction is f(r) only.

• Vertical hydrostatic equilibrium condition gives the same solutions for the lowest order in ϵ for the density (see Eq. 3.39), pressure and the sound speed as in the HD solution. The difference from KK00 is that now the disk surface boundary condition is not vacuum, but a corona with the density $\rho_{\rm cd}(r)$ at the disk interface. The zeroth order profile of density, pressure, and the sound speed are:

$$\rho_0(r,z) = \left[\rho_{\rm cd}^{2/3}(r) + \frac{h^2 - z^2}{5r^3}\right]^{3/2},$$

$$P_0(r,z) = \left[\rho_{\rm cd}^{2/3}(r) + \frac{h^2 - z^2}{5r^3}\right]^{5/2},$$

$$c_{s0}(r,z) = \sqrt{\frac{5}{3}\left[\rho_{\rm cd}^{2/3}(r) + \frac{h^2 - z^2}{5r^3}\right]}. \tag{3.66}$$

Clearly, $\rho_0(r,h) = \rho_{\rm cd}(r)$.

3.2.2 Analytical expressions from the numerical solutions

We verify if the results of our numerical simulations satisfy the obtained conditions.

Extensive numerical simulations with a KK00 disk as an initial condition were performed in [Čem19], following [ZF09]. Here we give a brief overview of the setup.

We solve the non-ideal MHD equations using the PLUTO (v.4.1) code [Mig+07] in the spherical grid. The resolution is $R \times \theta = (217 \times 100)$ grid cells, in a logarithmically stretched radial grid and in a half of the meridional half-plane in a uniform grid $\theta = [0, \pi/2]$. The viscosity and resistivity are parameterized by the [SS73] α-prescription as proportional to $c_{\rm s}^2/\Omega_{\rm K}$. For the magnetic field, a split-field method is used, so that we evolve in time only changes from the initial stellar magnetic field [Tan94; Pow+99], with the constrained transport method used to maintain the $\nabla \cdot \mathbf{B} = 0$. Simulations were performed using the second-order piecewise linear reconstruction and an approximate Roe solver. The second-order time-stepping (RK2) was employed.

Here we present the results in our HD and non-ideal MHD numerical simulations of a YSO, in the physical domain reaching 30 stellar radii, $R_{\rm max} = 30R_\star$, with the (anomalous[8]) viscosity parameter $\alpha_{\rm v} = 1$ and the mass accretion rate in the disk $\dot{M}_0 = 5 \times 10^{-7}\ M_\odot/{\rm yr}$. The stellar rotation rate is taken to be $\Omega_\star = 0.2\ \Omega_{\rm br}$, where $\Omega_{\rm br}$ is the equatorial mass-shedding limit rotation rate, equal to the Keplerian angular velocity for the star $\Omega_{\rm K\star} = \sqrt{GM_\star/R_\star^3}$. Thus, the corotation radius is $R_{\rm cor} = (GM_\star/\Omega_\star^2)^{1/3} = (0.2)^{-2/3}R_\star \approx 2.9R_\star$. In the Classical T-Tauri star case, the stellar mass is $M_\star = 0.5M_\odot$, radius $R_\star = 2R_\odot$, the Keplerian velocity

[8] Anomalous diffusive coefficients are much larger than their microscopic equivalent. They are usually given as free parameters in the simulations, assuming that dissipation is a result of turbulence.

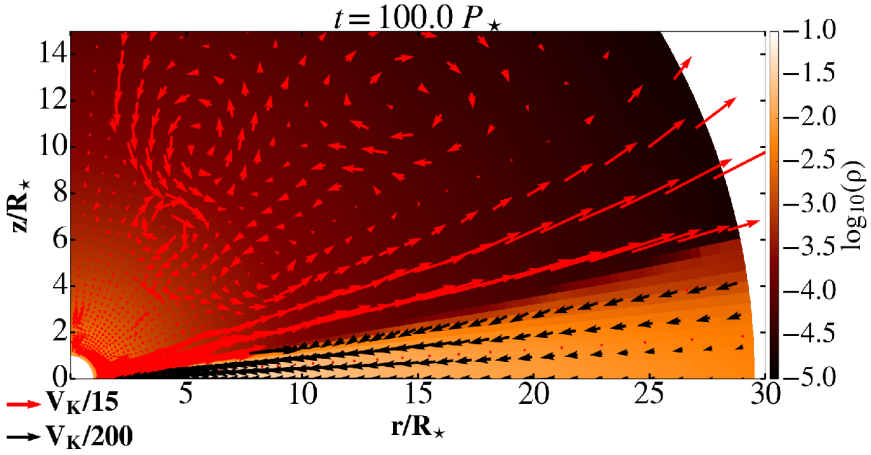

Figure 3.2: Capture of our hydrodynamic simulation after t=100 stellar rotations. The matter density is shown in logarithmic color grading in code units, with a sample of velocity vectors. Since the poloidal velocity in the corona is much larger than in the disk, velocity vectors are shown with a different scaling, as indicated by the arrows below the panel corresponding to multiples of the Keplerian velocity at the stellar surface.

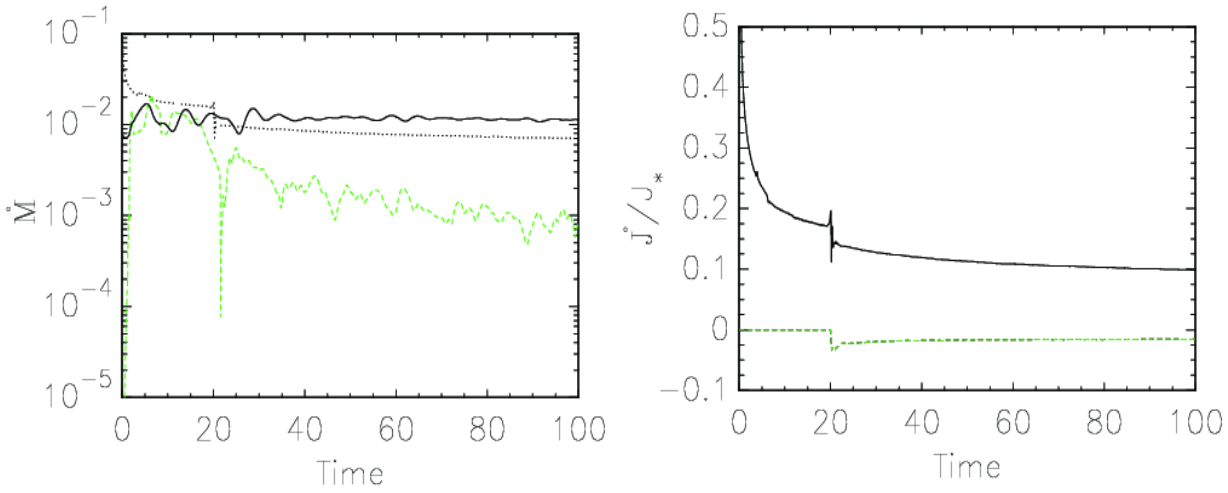

Figure 3.3: Illustration of the quasi-stationarity of our solution in the HD case. *Top panel:* evolution in time of the mass flux in the wind, onto the star and through the disk at r=15$R_\star$ (dashed green, dotted and solid lines, respectively), in units of $\dot{M}_0 = \rho_{\rm d0} R_\star^3 \Omega_{\rm K\star}$. *Bottom panel:* the torque exerted on the stellar surface by the matter accreted from the disk, and by the wind (solid and dashed green lines, respectively) in units of $\dot{J}_0 = \rho_{\rm d0} R_\star^5 \Omega_{\rm K\star}^2$ per stellar angular momentum $J_\star = k^2 M_\star R_\star^2 \Omega_\star$. For the typical normalized gyration radius of a fully convective star we use $k^2 = 0.2$. Positive torque spins-up, and negative torque spins-down the star. Time is measured in the number of stellar rotations.

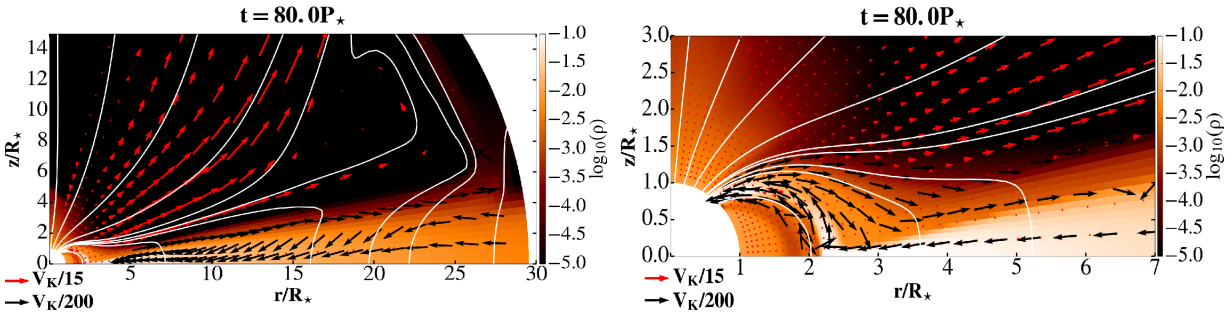

Figure 3.4: Captures of our magnetic simulation after t=80 stellar rotations (top panel), and a zoom closer to the star (bottom panel) to better show the accretion column. Colors and vectors have the same meaning as in Fig. 3.2. Note the different scale of the poloidal velocity (arrows below the panels). A sample of the poloidal magnetic field lines is shown with the solid lines.

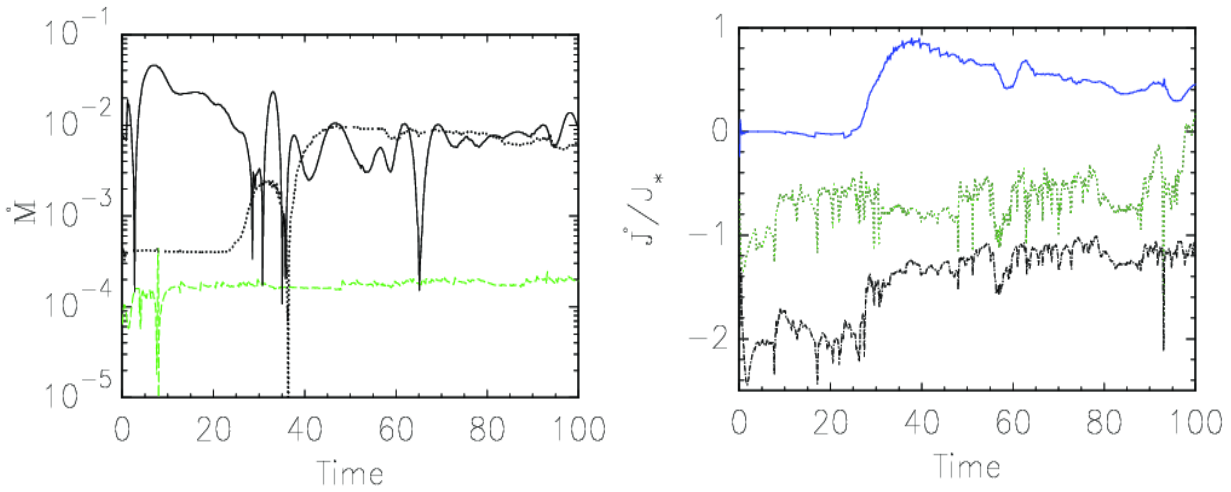

Figure 3.5: Illustration of the quasi-stationarity in our magnetic case solutions, in the same units as in Fig. 3.3. *Top panel:* the mass flux in the various components of the flow through the disk at r=15$R_\star$ (solid line), onto the stellar surface (dot-dashed line) and into the stellar wind (dashed green line). *Bottom panel:* the torques in the different components of the flow in the wind (dotted green line), in the matter falling onto the star from the part of the disk beyond $R_{\rm cor}$ (dot-dashed line) and below $R_{\rm cor}$ (solid blue line).

at the stellar equator is $v_{\mathrm{K}\star} = 218\ km/s$ and the stellar rotation period is $P_\star = 2\pi/\Omega_\star = 2.3$ days. Then $\rho_{\mathrm{d}0} = 1.2 \times 10^{-10} g/cm^3$. In the magnetic case we add the stellar dipole field of $B_\star = 500\ G$, and the resistivity parameter $\alpha_{\mathrm{m}} = 1$, so that the magnetic Prandtl number $P_{\mathrm{m}} = 2\alpha_{\mathrm{v}}/(3\alpha_{\mathrm{m}}) = 0.67$.

The assumed values of anomalous coefficients $\alpha_{\mathrm{v}} = \alpha_{\mathrm{m}} = 1$ are much larger than one would expect in an accretion disc. By such a choice we avoided changes in geometry of the flow: with $\alpha_{\mathrm{v}} < 0.685$ there is a backflow in the disk (see e.g. KK00 and [MČK20b] for a HD, and [MČK20a] for a MHD case), and with smaller values of α_{m} often a conical and/or axial outflows are launched from the magnetosphere [Kot+20].

A table for rescaling to other types of objects is given in [Čem19] where we performed a parameter study with the same set-up. We varied the stellar rotation rate, magnetic field strength and resistivity in the disk and compared the changes in results in dependence on those parameters.

We output the results along the z axis at two radial positions in the disk: in the middle of the radial domain, which lies far behind the distance r_m, where the viscous torque is vanishing[9] and closer to the star, just behind the corotation radius. We derive two sets of expressions along the vertical direction from those results, one at each distance from the star. Along the spherical radial direction, we output the results in the disk along a line near to the disk equator, and also along a line near to the disk surface. For each physical quantity, we verify if there is a unique solution throughout the disk.

Starting from the analytical solution as an initial condition in the simulations, we obtain a numerical solution. We then compare the quasi-stationary solutions in both the HD and the MHD solution, to the initial condition (i.e. the analytical solution) itself. The quasi-stationary solution does not change much in the final several tens of stellar rotations in our simulations. The magnetic field and the accretion rate of the observed stars are practically constant during such an interval, so that our time-independent analytical solutions are a good representation of the solutions.

Our computational domain reaches into the middle disk region, shown in Fig. 3.1, where the resistivity adds to the viscosity as a dissipation mechanism. This could make some of the assumptions from the purely HD disk implausible—we check whether or not this is true with the help of numerical simulations. We find that the magnetic solutions follow the HD solutions in the functional dependence, only the proportionality constants change.

A capture of our HD solution after 100 stellar rotations is shown in Fig. 3.2. The poloidal fluid velocity vectors are represented by the arrows, red for the corona, black for the disk, with a different scaling (one unit of arrow length corresponding to velocities in the corona and the disk in the ratio 40:3). In this case, accretion onto the star proceeds through the disk connected to the stellar equator. The mass and angular momentum fluxes onto the star and into the wind during the simulation are shown in Fig. 3.3.

The solution in the magnetic case is shown in Fig. 3.4. When the stellar dipole field is large enough, an accretion column is formed from the inner disk rim onto the stellar surface near the polar region. The matter is lifted above the disk equatorial plane, following the magnetic field lines. The mass flux onto the star and into the wind is shown in Fig. 3.5, together with the angular momentum fluxes, shown in the second panel in the same figure.

To investigate how much the magnetic solutions depart from the HD ones, and from the KK00 analytical solution, we directly compare the density and velocity profiles. Since the KK00 solutions are obtained in the cylindrical coordinates, which are more convenient to plot, we project our results from the simulations in spherical coordinates to the cylindrical coordinates. In all the cases we also show the closest match[10] to the case with $B_\star = 500$ G.

We can write the results in our simulations as simple functions obtained in KK00, with coefficients of

[9] The distance r_m defines a natural length scale $r_+ = \Omega_m^2 r_m^4/(GM_\star)$, with Ω_m the Keplerian rotation rate at r_m, see KK00. The outer region of the disk is at a much larger radius.

[10] Our approximate matches are not formal fits, but the simplest functions following the quasi-stationary solution. In most cases when the solution is without oscillations, the match is inside the 10% of the solution, as shown in Appendix. If oscillations are present, the error can be larger.

proportionality we find from our simulations:

$$\rho(r,z) = \frac{k_1}{r^{3/2}}\left[1-\left(\zeta_1\frac{z}{r}\right)^2\right]^{3/2}, \tag{3.67}$$

$$\begin{aligned} v_r(r,z) &= \frac{k_2}{r^{1/2}}\left[1+(\zeta_2 z)^2\right], \\ v_z(r,z) \approx \frac{z}{r}v_r(r,z) &= k_3\frac{z}{r^{3/2}}\left[1+(\zeta_3 z)^2\right], \\ v_\varphi(r,z) &= \frac{k_4}{\sqrt{r}},\ \Omega = \frac{v_\varphi}{r} = \frac{k_4}{r^{3/2}}. \end{aligned} \tag{3.68}$$

Magnetic field components are proportional to r^{-3}, as expected for the dipole stellar field, and depend linearly on height above the disk midplane:

$$B_r(r,z) = \frac{k_5}{r^3}z,\ B_z(r,z) = \frac{k_6}{r^3}z,\ B_\varphi(r,z) = \frac{k_7}{r^3}z, \tag{3.69}$$

In the case of B_r, the linear dependence is a consequence of the boundary condition at the disk equatorial plane, where the magnetic field components are reflected, with the change in sign of the component tangential to the boundary. This means that the radial magnetic field component $B_r \to 0$ at the equatorial plane, and is slowly increasing above (and below) that plane, in the densest parts of the disk. It is catching-up with more dramatic changes only close to the disk maximal height at the given radius, where it matches the values in the corona above the disk.

The vertical dependence of the viscous and resistive dissipative coefficients η and η_m in the initial conditions was taken to follow the $(z/r)^2$ dependence of $c_{\mathrm{s}0}^2$ from Eq. (3.66) in the analytical solution in Eq. (3.40), which can be further written as in Eq. (3.41). The same dependence is found in the results of our simulations, in both inner and outer parts of the disk:

$$\begin{aligned} \eta(r,z) &= \frac{k_8}{r}\left[1-\left(\zeta_8\frac{z}{r}\right)^2\right]^2, \\ \eta_\mathrm{m}(r,z) &= k_9\sqrt{r}\left[1-\left(\zeta_9\frac{z}{r}\right)^2\right]^{1/2}. \end{aligned} \tag{3.70}$$

We assign the proportionality coefficients as $k_1, k_2, \ldots$ in the cases with a stellar dipole field of 500 G and 1000 G in Table 3.1, indicating by the additional subscripts i and o if they are given in the *inner* (R=6) or *outer* (R=15) position in the disk. We also assign the corresponding coefficients $\zeta_1, \zeta_2, \ldots$ where needed.

In the following, we compare the above matches to solutions obtained in the simulations, with the conditions obtained from the analytical equations in the magnetic case.

3.3 Comparison of the analytical and numerical solutions

We show here the results in the cases of YSOs with the stellar magnetic field of 250, 500, 750 and 1000 G. In all the figures, shown are the approximate matching curves to the MHD solution in the case with the stellar field of 500 G.

When there are no oscillations in the solution, matching curves are mostly inside the 10 per cent error margin. When the oscillations are present, the error is larger. Functions are chosen to best match the values in the region of interest in the respective slices, even when it results in a larger error in the other parts of the approximated line.

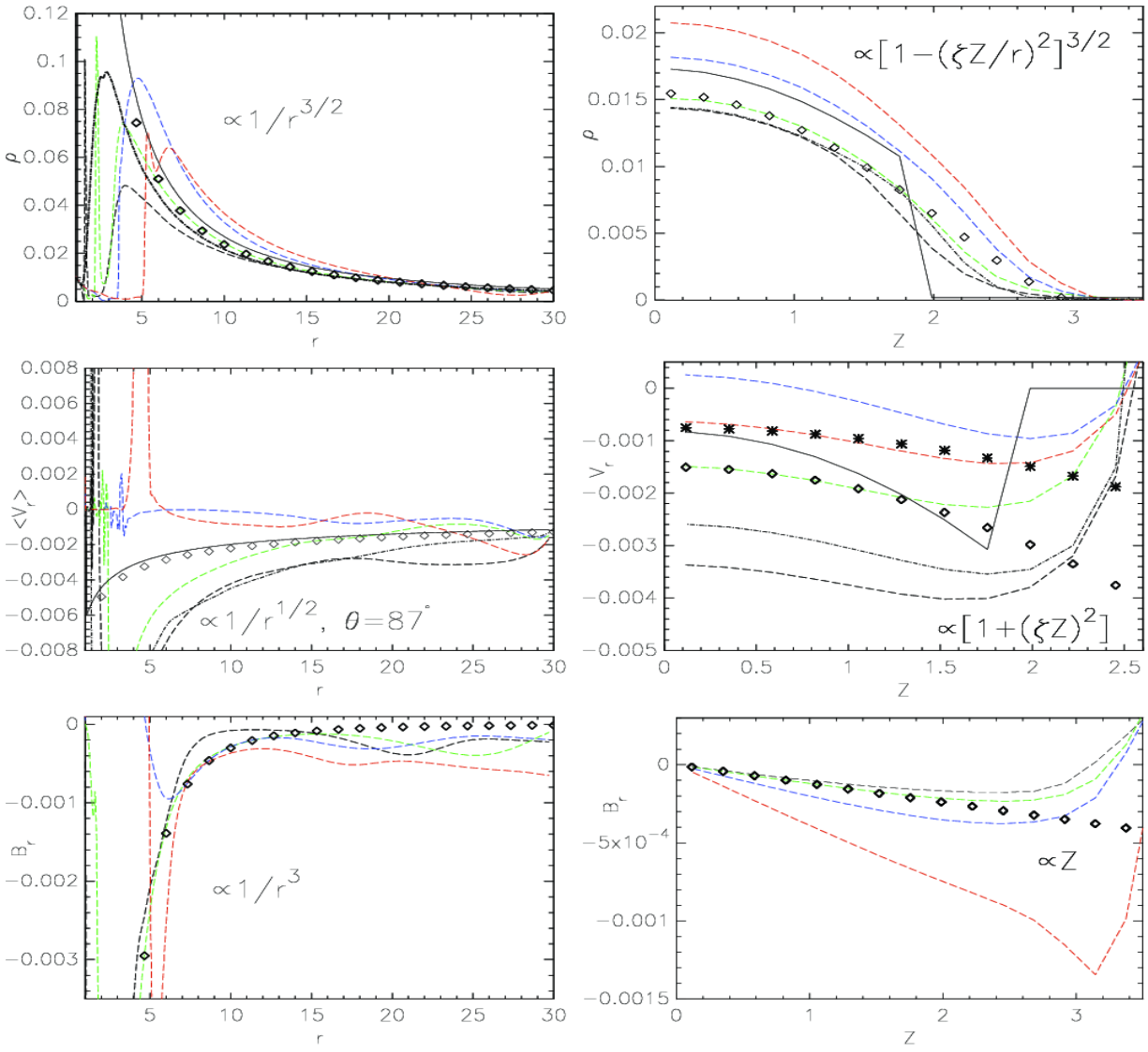

Figure 3.6: In the top panels are shown comparisons of the matter density in the initial set-up (thin solid line) with the quasi-stationary solutions in the numerical simulations in the HD (dot-dashed line) and the MHD (long-dashed line) cases, with Ω=0.2$\Omega_{\rm br}$. Left top panel: radial dependence along the midplane, just above θ=90°. Right top panel: the profiles along the vertical line at r=15$R_\star$. The HD and MHD profiles are nearly identical. In black, green, blue and red colors are the results in the MHD cases with the stellar magnetic field strengths 0.25, 0.5, 0.75 and 1.0 kG, respectively (from bottom to top along the line about the middle of the X-axis in both panels). The closest match to the 0.5 kG case is depicted with the diamond symbols. In the middle and bottom panels, with the same meaning of lines and symbols, are shown comparisons of the results for the radial velocity (the time-averaged radial components of the poloidal velocity are measured along the middle of the disk because of instability in a single time snapshots) and magnetic field components.

Table 3.1: The proportionality coefficients in our simulations with $B_\star$=0.5 kG and 1 kG.

B(kG)	0.5	1
coef.	R=6 — R=15	R=6 — R=15
k_{1i}—k_{1o}	0.9	1.2 — 0.29
k_{2i}—k_{2o}	-0.01 — -0.006	$+1.2\times10^{-4}$——2.9×10^{-3}
k_3	-2.65×10^{-4}	-4.4×10^{-3}——3.6×10^{-5}
k_4	0.255	0.255
k_{5i}—k_{5o}	-0.69 — -0.41	-1.25
k_{6i}—k_{6o}	-0.35 — -0.15	-0.29 — -0.19
k_{7i}—k_{7o}	-2.8 — -1.1	-8.2 — -1.18
k_8	5.8×10^{-3}	$8.\times10^{-3}$
k_9	0.01	0.01
ζ_1	5.	5.
ζ_2	0.5	0.5
ζ_8	5.	6.8
ζ_9	6.	4.5

We check now if the numerical solutions in the inner and outer disk regions are compatible with the conditions derived from the analytical equations. For the comparison, we use the expressions listed in the Eqs. (3.67-3.71).

Results for the radial dependence along a line just above the equatorial mid-plane of the disk, and for the vertical dependence along a line at r=15$R_\star$ show that the matching functions along the equatorial plane are of the same shape as along the disk surface at $\theta = 83°$. Also, the matching functions along a vertical direction closer to the star than r=15$R_\star$ are of the same shape as along a line further from the star, only the proportionality constants are different.

How do the obtained expressions compare to the general conditions obtained from the analytical equations?

• The numerical solution for the density in the magnetic case has the same dependence as the analytical one in the HD case. Both can be approximated by the same expression, with the difference only in the proportionality constant.

• The same is true for the velocity components, with the difference between the two numerical solutions most visible in the radial dependence in radial and vertical components of the poloidal velocity. The azimuthal velocity component does not change from the initial value since it is not evolved in our two-dimensional axisymmetric simulations.

• The magnetic field components in the disk in the simulations follow the expected $1/r^3$ decrease in the dipole field strength with distance from the star.

• In the analytical solution, all three magnetic field components are functions of r alone in the zeroth and first order in ϵ. With the nonvanishing magnetic field in the disk, and its vertical dependence on z, this leads to the conclusion that $\mathbf{B}_0$=0, and vertical, linear dependence on height above the disk equatorial plane should be related to the higher order in ϵ.

3.4 Difference between numerical and analytical solutions

Benefit of having a set of analytical expressions for the definition of accretion disk is in its universality in comparison with a particular numerical solution. In the theoretical work, in the initialization of the new numerical simulations, or post-processing of the simulations results, it is much simpler to refer to analytical

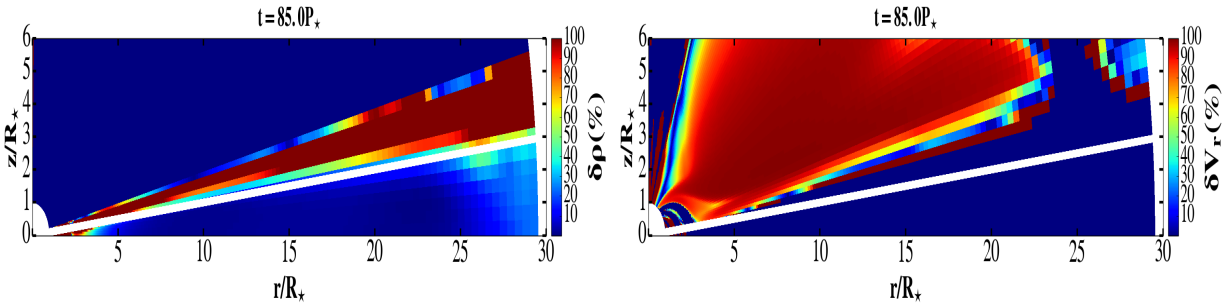

Figure 3.7: An example of difference between our numerical solutions and analytical expressions, in percentage of the value in the simulations. Our analytical solution is mostly inside the 10% margin everywhere inside the thin disk region, below the thick white solid line demarcating $h = 0.1r$ dependence, where h is the disk height. Close to the star and accretion column footpoint, our simulations are in the ideal MHD regime, so the analytical expressions fail there. It is also failing close to the outer boundary, where the material is fed into the disk by the amount based on the analytical solution in purely HD approach.

expression.

How different are our analytical expressions from the results in the simulations from which they are derived? We use the results computed with expressions from Eqs. (3.67-3.71) and coefficients from Table 3.1, to compute the difference for the physical quantities throughout the disk. The percentage of the value for the quantity Q from the simulation is:

$$\delta Q(\%) = 100 \frac{|Q_{sim} - Q_{an}|}{Q_{sim}}. \tag{3.71}$$

We show examples of this difference in Fig.3.7, the quasi-stationary result in a simulation with 500 G stellar field, and unit viscous and resistive coefficients α and $\alpha_{\rm m}$. In the thin disc, our analytical solutions for the density and velocity components are inside the 10% margin. Similar results hold for the viscosity η and resistivity $\eta_{\rm m}$. Between the star and accretion column footpoint our simulations are in the ideal MHD regime, and close to the outer boundary the material is fed into the disk as prescribed from the HD results. Our analytical expressions are derived inside the middle disk region, so they fail in both those regions, as expected.

Bibliography

[BH91] Steven A. Balbus and John F. Hawley. *A Powerful Local Shear Instability in Weakly Magnetized Disks. I. Linear Analysis*. 376 (July 1991), p. 214 (cit. on p. 12).

[Bon52] H. Bondi. *On spherically symmetrical accretion*. 112 (Jan. 1952), p. 195 (cit. on p. 9).

[Čem19] M. Čemeljić. *"Atlas" of numerical solutions for star-disk magnetospheric interaction*. 624, A31 (Apr. 2019), A31. arXiv: 1811.02808 [astro-ph.SR] (cit. on pp. 38, 41).

[ČPK18] Miljenko Čemeljić, Varadarajan Parthasarathy, and Włodek Kluźniak. *Analytical solution for magnetized thin accretion disk in comparison with numerical simulations*. arXiv e-prints, arXiv:1812.09132 (Dec. 2018), arXiv:1812.09132. arXiv: 1812.09132 [astro-ph.SR] (cit. on p. 27).

[F J53] F. J. S. *The Earth; its origin, history and physical constitution. By Harold Jeffreys, F.R.S. Cambridge (University Press), 1952. 3rd Edition. Pp. xi, 392; 10 plates, 30 Figs. 70s*. Quarterly Journal of the Royal Meteorological Society 79.340 (Apr. 1953), pp. 309–309 (cit. on p. 12).

[FKR02] Juhan Frank, Andrew King, and Derek J. Raine. *Accretion Power in Astrophysics: Third Edition*. 2002 (cit. on p. 18).

[Hōs77] R. Hōshi. *Basic Properties of a Stationary Accretion Disk Surrounding a Black Hole*. Progress of Theoretical Physics 58.4 (Oct. 1977), pp. 1191–1204 (cit. on p. 33).

[HS70] George H. Herbig and Otto Struve. *Spectroscopic astrophysics. an assessment of the contributions of Otto Struve*. 1970 (cit. on pp. 5, 7).

[Hua63] Su-Shu Huang. *An Interpretation of Beta Lyrae*. 138 (Aug. 1963), p. 342 (cit. on p. 7).

[Kit95] David B. Kita. "A Study of the Vertical and Radial Structure of Polytropic Accretion Disks". PhD thesis. THE UNIVERSITY OF WISCONSIN - MADISON., Jan. 1995 (cit. on p. 26).

[KK00] W. Kluzniak and D. Kita. *Three-dimensional structure of an alpha accretion disk*. arXiv e-prints, astro-ph/0006266 (June 2000), astro–ph/0006266. arXiv: astro-ph/0006266 [astro-ph] (cit. on p. 26).

[Kot+20] Aleksandra Kotek et al. *Asymmetric Jet launching*. XXXIX Polish Astronomical Society Meeting. Ed. by Katarzyna Małek et al. Vol. 10. Oct. 2020, pp. 275–278. arXiv: 2006.04083 [astro-ph.HE] (cit. on p. 41).

[Lyn69] D. Lynden-Bell. *Galactic Nuclei as Collapsed Old Quasars*. 223.5207 (Aug. 1969), pp. 690–694 (cit. on p. 18).

[MČK20a] Ruchi Mishra, Miljenko Čemeljić, and Wlodek Kluźniak. *Backflow in simulated MHD accretion disks*. arXiv e-prints, arXiv:2012.13194 (Dec. 2020), arXiv:2012.13194. arXiv: 2012.13194 [astro-ph.SR] (cit. on p. 41).

[MČK20b] Ruchi Mishra, Miljenko Čemeljić, and Włodek Kluźniak. *Backflow in Accretion Disk*. XXXIX Polish Astronomical Society Meeting. Ed. by Katarzyna Małek et al. Vol. 10. Oct. 2020, pp. 147–150. arXiv: 2006.01851 [astro-ph.SR] (cit. on p. 41).

[Mig+07] A. Mignone et al. *PLUTO: A Numerical Code for Computational Astrophysics*. 170 (May 2007), pp. 228–242. eprint: astro-ph/0701854 (cit. on p. 38).

[Mis+20] Bhupendra Mishra et al. *Strongly magnetized accretion discs: structure and accretion from global magnetohydrodynamic simulations*. 492.2 (Feb. 2020), pp. 1855–1868. arXiv: 1907.08995 [astro-ph.HE] (cit. on p. 12).

[NY95] Ramesh Narayan and Insu Yi. *Advection-dominated Accretion: Underfed Black Holes and Neutron Stars*. 452 (Oct. 1995), p. 710. arXiv: astro-ph/9411059 [astro-ph] (cit. on p. 26).

[Pow+99] K. G. Powell et al. *A Solution-Adaptive Upwind Scheme for Ideal Magnetohydrodynamics*. Journal of Computational Physics 154 (Sept. 1999), pp. 284–309 (cit. on p. 38).

[Pri81] J. E. Pringle. *Accretion discs in astrophysics*. 19 (Jan. 1981), pp. 137–162 (cit. on p. 25).

[Reb+09] P. Rebusco et al. *Global transient dynamics of three-dimensional hydrodynamical disturbances in a thin viscous accretion disk*. Physics of Fluids 21.7 (July 2009), pp. 076601–076601. arXiv: 0906.0004 [astro-ph.HE] (cit. on pp. 28, 30).

[Reg83] O. Regev. *The disk-star boundary layer and its effect on the accretion disk structure*. 126.1 (Sept. 1983), pp. 146–151 (cit. on p. 25).

[SS73] N. I. Shakura and R. A. Sunyaev. *Black holes in binary systems. Observational appearance*. 24 (Jan. 1973), pp. 337–355 (cit. on pp. 12, 17, 18, 38).

[Tan94] T. Tanaka. *Finite volume TVD scheme on an unstructured grid system for three-dimensional MHD simulation of inhomogeneous systems including strong background potential fields*. Journal of Computational Physics 111 (Apr. 1994), pp. 381–390 (cit. on p. 38).

[Urp84] V. A. Urpin. *Hydrodynamic flows in accretion disks*. 61 (Feb. 1984), pp. 84–90 (cit. on p. 25).

[Wei48] Carl Friedrich Weizsäcker. *Die Rotation kosmischer Gasmassen*. Zeitschrift Naturforschung Teil A 3 (Nov. 1948), pp. 524–539 (cit. on p. 12).

[ZF09] C. Zanni and J. Ferreira. *MHD simulations of accretion onto a dipolar magnetosphere. I. Accretion curtains and the disk-locking paradigm*. 508.3 (Dec. 2009), pp. 1117–1133 (cit. on p. 38).